Tutorial Review

Thermodynamic and Kinetic Hydricity of Transition Metal Hydrides

Kelsey R. Brereton,[a,‡] Nicholas E. Smith,[b,‡] Nilay Hazari,[b,*] Alexander J. M. Miller[c,*]

[a] Department of Chemistry, Pepperdine University, Malibu, California, 90263, USA

[b] Department of Chemistry, Yale University, P. O. Box 208107, New Haven, Connecticut, 06520, USA

[c] Department of Chemistry, University of North Carolina at Chapel Hill, Chapel Hill, North Carolina, 27599-3290, USA

Abstract

The prevalence of transition metal-mediated hydride transfer reactions in chemical synthesis, catalysis, and biology has inspired the development of methods for characterizing the reactivity of transition metal hydride complexes. Thermodynamic hydricity represents the free energy required for heterolytic cleavage of the metal–hydride bond to release a free hydride ion, H^-, as determined through equilibrium measurements and thermochemical cycles. Kinetic hydricity represents the rate of hydride transfer from one species to another, as measured through kinetic analysis. This tutorial review describes the common methods for experimental and computational determination of thermodynamic and kinetic hydricity, including advice on best practices and precautions to help avoid pitfalls. The influence of solvation on hydricity is emphasized, including opportunities and challenges arising from comparisons across several different solvents. Connections between thermodynamic and kinetic hydricity are discussed, and opportunities for utilizing these connections to rationally improve catalytic processes involving hydride transfer are highlighted.

Key Learning Points Box

- Thermodynamic hydricity, the free energy required to release a free hydride ion from a species, is determined using thermochemical cycles. Experimental free energies needed for the thermochemical cycles come from equilibrium studies, which are only accurate when a true equilibrium is established.

- Kinetic hydricity is determined by measuring the rate of hydride transfer using kinetics. It is important to confirm the identity of the products and ensure that a rate constant describing the elementary hydride transfer step can be extracted from the data.
- Solvent effects are important in both thermodynamic and kinetic hydricity. They must be considered when making comparisons of values and can provide insight into the nature of transition states for hydride transfer.
- Thermodynamic and kinetic hydricity are valuable tools for understanding individual hydride transfer reactions, especially for applications in catalysis. When hydride transfer is the turnover-limiting step in a catalytic reaction, linear-free energy relationships can guide catalyst design choices.

Correspondence

N.H.: nilay.hazari@yale.edu

A.J.M.M.: ajmm@email.unc.edu

Author Notes

‡ These authors contributed equally.

I. Introduction

Hydride transfer reactions are prevalent in the chemical sciences, with diverse applications in areas including biochemistry, organic synthesis, homogeneous catalysis, and alternative energy conversion. Transition metal hydride complexes are key intermediates in many of these reactions. Therefore, there is significant interest in developing methods to elucidate mechanistic insight into hydride transfer reactions, with a focus on understanding how to improve hydride transfer reactivity by changing the structure of the hydride donor or by altering the reaction conditions.

Hydricity is a measure of the propensity of a species to transfer a hydride ion. Two distinct approaches to establishing hydricity have developed over the past 50 years, as illustrated in Figure 1. In analogy to acid-base terminology, both approaches adopt the nomenclature of "hydride donor" for the species that transfers a hydride ion and "conjugate hydride acceptor" for the species formed upon removal of H^-.

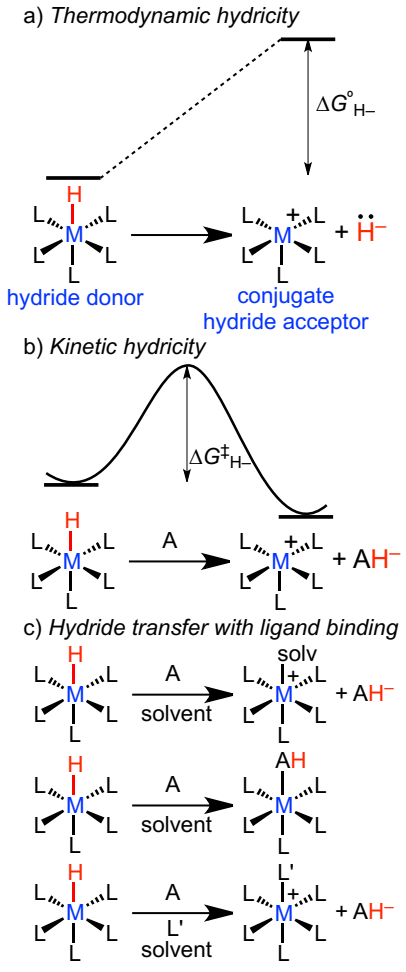

Figure 1. Reaction coordinate diagrams illustrating the reactions associated with thermodynamic hydricity, ΔG^{o}_{H-} **(a)**, and kinetic hydricity, $\Delta G^{\ddagger}_{H-}$ **(b)**, which depends on the specific acceptor used, A. Special consideration is necessary when hydride transfer is accompanied by association of solvent, product, or another ligand **(c)**.

Thermodynamic hydricity is the free energy required to release a free hydride ion, H^-, from a species in solution (ΔG^{o}_{H-}, Figure 1a), including non-specific solvation effects as well as the energy of any solvent binding to the metal center (Figure 1c). If a ligand other than solvent binds after hydride transfer (Figure 1c), an *effective thermodynamic hydricity* can be calculated, which is the sum of the thermodynamic hydricity and the free energy of ligand binding. There are several methods to experimentally determine the thermodynamic hydricity of a hydride donor, each based on one or more equilibrium measurements. Thermodynamic hydricity is attractive because it represents an "absolute" scale, and is related to other bond strength parameters (e.g. bond dissociation free energy, BDFE) that are often used to build linear free energy relationships. It has limitations as well, particularly the issue of invoking the free hydride ion, which is not stable in solution, in a solution-phase thermodynamic parameter.

Kinetic hydricity is the relative rate of hydride transfer from a hydride donor to a hydride acceptor. This is usually taken to mean the elementary rate constant of the hydride transfer reaction (related to the activation energy $\Delta G^{\ddagger}_{H-}$, Figure 1b). A kinetic hydricity scale is constructed by measuring the relative rates of hydride transfer from several hydride donors to the same hydride acceptor under identical conditions. The measurement of kinetic hydricity is attractive because it directly measures the hydride transfer rate constant. The limitations of kinetic hydricity include the inherent difficulty of kinetic measurements as well as the possibility that the measured hydride transfer kinetics may not be directly applicable to hydride transfer to other substrates.

There are several excellent reviews on hydricity, including comprehensive articles on the thermodynamic hydricity of transition metal hydrides and the thermodynamic and kinetic hydricity of metal-free hydride donors.[1–5] In this Tutorial Review, we provide an overview of the experimental and computational methods for determining both the thermodynamic and kinetic hydricity of transition metal hydrides. Successful strategies in experimental design and common pitfalls to avoid are described. A particular emphasis is placed on the effect of solvent on hydricity, which has recently emerged as a critical parameter. Finally, we provide case studies that illustrate how thermodynamic and kinetic hydricity parameters can guide catalyst development.

II. Thermodynamic hydricity

Introduction

This section provides a tutorial on how to determine thermodynamic hydricity in a wide range of solvents, followed by case studies of catalyst design guided by hydricity, and our opinions on current challenges and future research directions. There are several experimental and computational methods for hydricity determination. The experimental methods rely on estimates of thermodynamic parameters that relate the species H^+, H^-, and H_2. While the absolute precision of these parameters can be questionable, the adoption of a single value for each solvent provides an accurate relative scale. The ability to compare the heterolytic bond strength associated with the release of H^- is one of the most valuable aspects of thermodynamic hydricity, enabling predictions of the thermodynamic favorability of a wide array of hydride transfer reactions. These predictions can form the basis of catalyst design strategies.

Experimental determination of thermodynamic hydricity

Thermochemical background. There are three primary methods to determine thermodynamic hydricity that have been described as the "potential–pK_a" method, the "H_2 heterolysis" method, and the "hydride transfer" method.[2] The first two methods can be measured independently, without the need for a reference species of known hydricity. Instead, they rely on thermodynamic parameters that describe the free energy of H^+ reduction to H^- (for the potential–pK_a method) or the free energy to heterolytically split H_2 into H^+ and H^- (for the H_2 heterolysis method). These thermodynamic parameters are often referred to as "constants" because specific values are employed for all hydricity determinations in a particular solvent, but these values are unique to each solvent because differences in solvation lead to differences in free energy of reactions involving H^+, H^-, and H_2. The adopted solvent-specific parameters, which represent best estimates derived from available experimental parameters at standard state conditions of 1 M solutes, 1 atm gases, 298 K, and constant solvent activity, are presented in the following paragraphs.

The free energy of H^+ reduction to H^- ($\Delta G^\circ_{H+/H-}$) and the free energy of H_2 splitting to H^+ and H^- (ΔG°_{H2}) are presented in Table 1 in different organic solvents and in water. Remarkably, all of these thermodynamic parameters can be derived from just three *aqueous* reduction potentials (see ESI for details): (1) the reduction of H^+ to H_2, the normal hydrogen electrode potential (E° =

0 V vs. NHE), (2) the reduction of H^+ to free hydrogen atom, H• ($E^o_{H+/H•}$ = –2.29 V vs. NHE), and (3) the reduction of H• to H^- ($E^o_{H•/H-}$ = +0.81 V vs. NHE). The currently accepted values for each reaction are highlighted here. $\Delta G^o_{H+/H-}$ and ΔG^o_{H2} are related by the standard reduction potential of H^+ to form H_2, $E^o_{H+/H2}$. In water, $E^o_{H+/H2}$ is 0 V vs. NHE, so $\Delta G^o_{H+/H-}$ and ΔG^o_{H2} are identical.

Table 1. Free energies of H_2 heterolysis (ΔG^o_{H2})[6–9] and H^+ reduction to H^- ($\Delta G^o_{H+/H-}$) in various solvents.

Reaction	$H_2 \rightleftarrows H^+ + H^-$	$H^+ + 2e^- \rightleftarrows H^-$
	ΔG^o_{H2} (kcal/mol)	$\Delta G^o_{H+/H-}$ (kcal/mol)
Water	**34.2**	**34.2**
Acetonitrile	76.0[a]	79.6[a,b]
N,N-Dimethylformamide	55.4	86.1[b]
Dimethyl sulfoxide	60.7[a]	71.4
Ethanol	45.4	85.6
Ethylene glycol	41.6	76.9
Methanol	43.3	89.4
N-methyl-2-pyrrolidone	—	74.6
Tetrahydrofuran	68.7	84.3[b]

[a] Derived using different values for aqueous free energies, see main text for details. [b] Based on Scheme S2 in ESI using $E^o_{H+/H2}$.

In organic solvents, the parameters in Table 1 were obtained through the thermochemical cycles shown in Schemes 1 and 2. To determine ΔG^o_{H2} in organic solvents according to Scheme 1, the free energies to transfer H^+ and H^- from water to the organic solvent of interest ($\Delta G^o_{tr}(H^+)$ and $\Delta G^o_{tr}(H^-)$, respectively) are needed.[9] Good estimates for $\Delta G^o_{tr}(H^+)$ are available for a range of relatively polar solvents.[9] Due to the fact that the free hydride ion is unstable, values for $\Delta G^o_{tr}(H^-)$ must be estimated, in this case by extrapolation of the transfer free energies of the halides.[7] The method of Scheme 1 should utilize the currently adopted aqueous value for ΔG^o_{H2}, 34.2 kcal/mol, which would enable construction of hydricity scales that are internally consistent across solvents from this single aqueous thermodynamic parameter. However, it is important to emphasize that the currently employed hydricity scales *are not internally consistent across solvents,* because the acetonitrile and dimethyl sulfoxide hydricity scales were originally constructed using a different

aqueous value for $E^{o}_{H\bullet/H^-}$ (0.18 V vs NHE instead of 0.81 V vs NHE, which was used for all other solvents in Table 1).[6,8] Re-deriving the acetonitrile scale using $E^{o}_{H\bullet/H^-}$ = 0.81 V vs NHE reveals that differences in hydricity between acetonitrile and water are artificially inflated by a constant value of 13.75 kcal/mol (12.6 kcal/mol for dimethyl sulfoxide and water).[9] The impact of this unfortunate scenario is the *illusion* that hydrides *appear to be* much stronger hydride donors in water than in acetonitrile. We now understand that this difference is more modest, as can be seen in Figure 8 below. Apart from this illusion, however, the currently employed thermodynamic parameters are adequate in developing hydricity values that enable chemists to understand and predict reactivity: the relative ordering of hydride donor abilities in any particular solvent is unaffected by the choice of thermodynamic parameter. As such, we report the long-used acetonitrile constants and the recently reported dimethyl sulfoxide constants in Table 1, but emphasize to the community that care should be taken when making general comparisons or predictions across solvents. Further, experimental/computational methods are available for predicting changes in solvent that correct for different scale conventions (see below).[9]

Scheme 1. Thermochemical cycle used to obtain the free energy of H_2 heterolysis, ΔG^{o}_{H2}, in organic solvents (solv).

$H_{2(g)} \rightleftarrows H^+_{(aq)} + H^-_{(aq)}$	ΔG^{o}_{H2} in H_2O	(1)
$H^-_{(aq)} \rightleftarrows H^-_{(solv)}$	$\Delta G^{o}_{tr}(H^-)$	(2)
$H^+_{(aq)} \rightleftarrows H^+_{(solv)}$	$\Delta G^{o}_{tr}(H^+)$	(3)
$H_{2(g)} \rightleftarrows H^+_{(solv)} + H^-_{(solv)}$	ΔG^{o}_{H2} in solv	(4)

Scheme 2. Thermochemical cycle used to obtain the free energy of H^+ reduction to H^-, $\Delta G^{o}_{H+/H-}$, in organic solvents (solv).

$H^+_{(aq)} + 2e^-_{NHE} \rightleftarrows H^-_{(aq)}$	$\Delta G^{o}_{H+/H-}$ in H_2O	(5)
$H^-_{(aq)} \rightleftarrows H^-_{(solv)}$	$\Delta G^{o}_{tr}(H^-)$	(6)
$H^+_{(solv)} \rightleftarrows H^+_{(aq)}$	$-\Delta G^{o}_{tr}(H^+)$	(7)
$2e^-_{Fc} \rightleftarrows 2e^-_{NHE}$	Ref. electrode correction	(8)
$H^+_{(solv)} + 2e^-_{Fc} \rightleftarrows H^-_{(solv)}$	$\Delta G^{o}_{H+/H-}$ in solv	(9)

To determine $\Delta G^{o}_{H+/H-}$ in organic solvents according to Scheme 2, $\Delta G^{o}_{tr}(H^+)$ and $\Delta G^{o}_{tr}(H^-)$ are needed, along with a reference electrode correction to move from NHE in water to the

ferrocenium/ferrocene (Fc^+/Fc) reference potential in the organic solvent of interest (Scheme 2). An alternative derivation is possible if $E^o_{H+/H2}$ has been measured in the organic solvent of interest, as described in the ESI. Table 1 shows $\Delta G^o_{H+/H-}$values for nine solvents. The values of $\Delta G^o_{H+/H-}$ in water and acetonitrile have been reported previously and are widely used to determine hydricity. Seven other sets of constants are presented here for the first time, derived using the approach of Savéant and Gennaro (except N,N-dimethylformamide and THF, where $E^o_{H+/H2}$ is available, see ESI for details).[10,11] Sources of uncertainty in the $\Delta G^o_{H+/H-}$ values are discussed in the ESI. As long as the same $\Delta G^o_{H+/H-}$ values are used by the research community for hydricity determination, the scale will be self-consistent and facilitate comparisons of relative hydricity between complexes in each solvent. Note that, unlike in water, $\Delta G^o_{H+/H-}$ and ΔG^o_{H2} differ by the free energy of $E^o_{H+/H2}$ (V vs $Fc^{+/0}$) in organic solvents (Table 1).

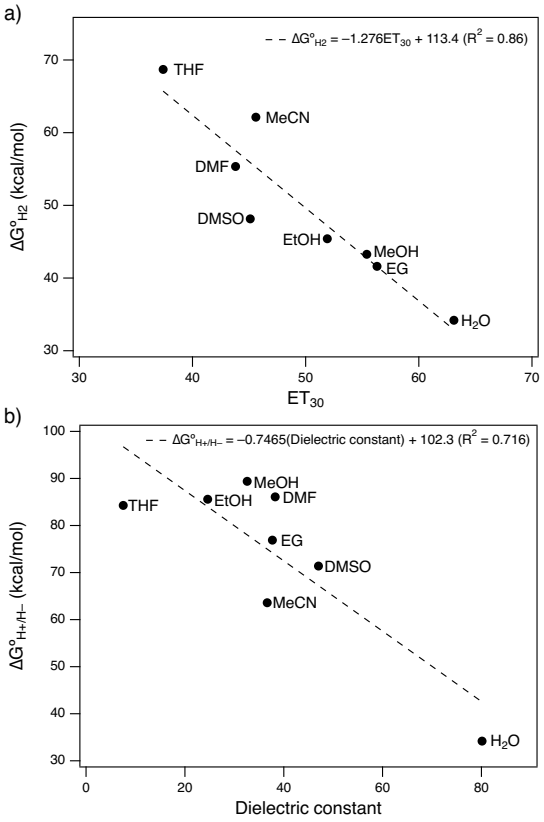

Figure 2. Correlations between ΔG^o_{H2} and ET_{30} **(a)** and $\Delta G^o_{H+/H-}$ and dielectric constant **(b)**. Linear fits shown in dashed lines. See ESI for correlations with other solvent parameters.

To understand the influence of solvent on the two thermodynamic parameters ΔG^o_{H2} and $\Delta G^o_{H+/H-}$, correlations were sought with four commonly employed solvent parameters. Plots against dielectric constant, acceptor number, donor number, and the Dimroth-Reichart parameter

for photoelectronic excitation (ET_{30}) are shown in the ESI. For ΔG^{o}_{H2}, the strongest correlation was observed with ET_{30} (Figure 2a), perhaps reflecting solvation of a cation/anion pair (Reichart's dye is zwitterionic). In contrast, $\Delta G^{o}_{H+/H-}$ showed the strongest correlation with dielectric constant (Figure 2b). These empirical correlations may be useful for predicting properties related to hydricity in new solvents.

Knowledge of the required thermodynamic parameters allows us to discuss techniques for experimentally determining thermodynamic hydricity in more detail. The methods have been reviewed previously.[2] A brief tutorial covering the methods is included here for pedagogical reasons, and details on best practices are emphasized.

Potential–pK_a method. The "potential–pK_a" method involves experimentally measuring the pK_a of the metal hydride and the two 1e$^-$ reduction potentials of the conjugate hydride acceptor (Figure 3 and Scheme 3). This method is distinct from the other two because it requires access to the conjugate base of the hydride. The metal hydride complex must be sufficiently acidic that it can be deprotonated more readily than the solvent. If the hydride can indeed be deprotonated, the conjugate base must then be stable and soluble under the desired reaction conditions. There are numerous methods available for the determination of hydride acidity.[12] The unitless pK_a value is converted to a free energy at 298 K, with units of kcal/mol, by multiplying 1.364·pK_a. Two 1e$^-$ reductions of the conjugate hydride acceptor generate the conjugate base of the hydride, so the stability requirements discussed above also apply to reduction potential measurements. The reduction potentials are most commonly obtained using cyclic voltammetry. In organic solvents, potentials (in volts) are reported against the ferrocenium/ferrocene (Fc^+/Fc) reference potential; in water, potentials are reported against NHE. 1e$^-$ reduction potentials can be converted to free energies at 298 K (in kcal/mol) by multiplying –23.06·E^o (doubled for a 2e$^-$ reduction). Thermodynamic hydricity values obtained from this method typically have uncertainties of approximately ±1 kcal/mol, with the error associated primarily with uncertainty in the reduction potentials.

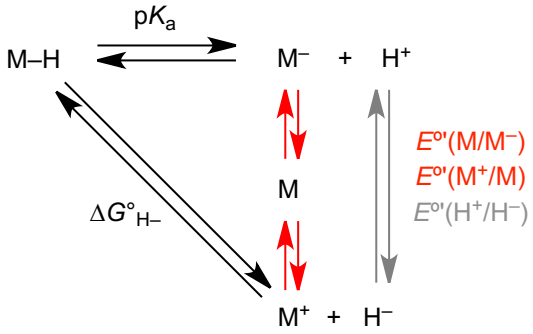

Figure 3. Thermochemical scheme for determining thermodynamic hydricity using the potential–pK_a method.

Scheme 3. Thermochemical cycle for determining thermodynamic hydricity using the potential–pK_a method at 298 K.

$MH \rightleftarrows M^- + H^+$	$\Delta G^o = 1.364 \cdot pK_a$	(10)
$M^- \rightleftarrows M^0 + e^-$	$\Delta G^o = 23.06 \cdot E^o$	(11)
$M^0 \rightleftarrows M^+ + e^-$	$\Delta G^o = 23.06 \cdot E^o$	(12)
$H^+ + 2e^- \rightleftarrows H^-$	$\Delta G^o_{H+/H-} = 23.06 \cdot E^o_{H+/H-}$	(13)
$MH \rightleftarrows M^+ + H^-$	ΔG^o_{H-}	(14)

H_2 heterolysis method. The "H_2 heterolysis" method involves establishing equilibrium between the conjugate hydride acceptor, a base, and H_2, giving detectable amounts of the metal hydride of interest and the conjugate acid. This provides the relative hydricity of the metal hydride compared to H_2, which has a known hydricity value (ΔG^o_{H2}) in many solvents (Table 1). The pK_a of the conjugate acid in the solvent of interest must also be known to complete the thermochemical cycle (Scheme 4). The H_2 heterolysis method is perhaps the most commonly employed form of hydricity determination. It only requires synthetic access to the conjugate hydride acceptor, which is often more stable than the hydride itself, and it can be performed in a sealed NMR tube under 1 atm of H_2.

Scheme 4. Thermochemical cycle for determining thermodynamic hydricity using the H_2 heterolysis method.

$MH + H\text{–}Base^+ \rightleftarrows M^+ + H_2 + Base$	$\Delta G^o = -1.364 \cdot \log(K_{eq})$	(15)
$H^+ + Base \rightleftarrows H\text{–}Base^+$	$\Delta G^o = -1.364 \cdot pK_a$	(16)
$H_2 \rightleftarrows H^+ + H^-$	ΔG^o_{H2}	(17)
$MH \rightleftarrows M^+ + H^-$	ΔG^o_{H-}	(18)

Hydride Transfer Method. The "hydride transfer" method involves establishing an equilibrium between two hydride donor/conjugate acceptor pairs, one of unknown hydricity and one of known hydricity ("reference" hydride donor HA^-, Figure 4 and Scheme 5). The experiment can be performed by allowing a hydride of unknown hydricity to react with a reference acceptor, or by allowing a reference hydride to react with the conjugate hydride acceptor of the species of unknown hydricity. NMR spectroscopy is a convenient method for monitoring these reactions because the chemical shifts of hydride complexes are usually distinct. However, any spectroscopic method where the various reactants and products can be quantified is suitable. For NMR spectroscopy, the typical sensitivity allows for the equilibrium to be measured if the hydride donor/conjugate acceptor pairs are within approximately 3 kcal/mol of each other. This method is particularly attractive for rapidly determining hydricity for related complexes, which often have similar hydricity and rarely encounter stability or incompatibility problems. Relative hydricity values determined using these methods are often quantifiable to within ±0.1 kcal/mol.

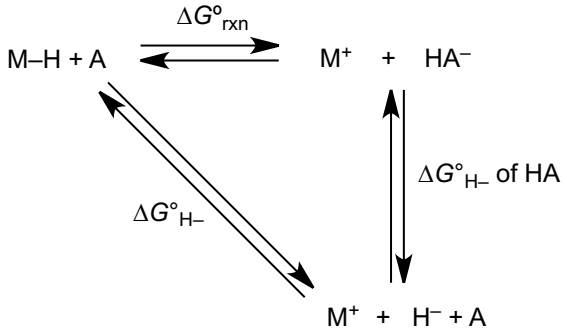

Figure 4. Thermochemical scheme for determining thermodynamic hydricity using the hydride transfer method.

Scheme 5. Thermochemical cycle for determining thermodynamic hydricity using the hydride transfer method.

$MH + A \rightleftarrows M^+ + HA^-$	$\Delta G^\circ = -1.364 \cdot \log(K_{eq})$	(19)
$HA^- \rightleftarrows A + H^-$	ΔG°_{H-} of HA^-	(20)
$MH \rightleftarrows M^+ + H^-$	ΔG°_{H-} of MH	(21)

For all three methods, there are several experimental factors to consider. It is critical to ensure that equilibrium is established for any experimental measurements. Only systems at equilibrium accurately represent the chemical thermodynamics. Confirmation of true equilibrium can be obtained by (a) ensuring that concentrations change over time initially before approaching constant values, (b) approaching equilibrium from both directions (either in two separate reactions,

or by adding reagents to reverse the reaction as in a reverse titration), and/or (c) perturbing the system and allowing it to return to equilibrium (for example, by adding more of one reactant). Reduction potentials are only equilibrium quantities when the reduction feature is fully reversible (the assumption $E_{1/2} = E^{o}$ is only valid for reversible features). Chronoamperometry or redox titrations have been used successfully and may also be appropriate,[13] as long as the reduction is chemically reversible. In reactions involving gases, the pressure should be constant during the experiment, which sometimes requires backfilling the vessel periodically. Gas mixing can also be an important factor to consider, especially in solvents with poor gas solubility.

The choice of solvent can be critical. The solvent should have a well-defined hydricity scale to enable meaningful comparisons with other hydride donor/conjugate acceptor pairs. All of the species involved must be soluble in the solvent employed (including the conjugate base of the hydride complex, if the potential–pK_a method is to be employed), as precipitation prevents measurement of the desired equilibrium. The ability of the solvent to act as a ligand should be considered, as many complexes bind a solvent after hydride transfer (see Figure 1c above). Although this is considered part of the overall solvation and is therefore accounted for in the thermochemical cycles, it can complicate the experiments. More broadly, it is important to confirm the identity of all reaction products to ensure that the thermochemical cycle is properly balanced (accounting for any ligand association/dissociation events, for example). For the potential–pK_a method, the solvent must also dissolve an appropriate electrolyte to carry out the electrochemical measurements. This also raises the possibility of additional electrolyte effects; to maintain an identical medium, the pK_a titration should also be carried out in electrolyte, and subtle differences in hydricity using different methods could possibly be due to electrolyte effects.

Computational methods for determining thermodynamic hydricity

There are four general methods for the computational determination of thermodynamic hydricity. A direct computation of the M–H heterolytic bond strength uses an estimation for the energy of a solvated hydride ion. The three other methods are analogous to the experimental methods described above.

The direct computation of M–H heterolysis requires computing the free energy of the hydride complex, its conjugate acceptor, and the solvated free hydride ion. This strategy is attractive because it is a calculation of the precise reaction that represents thermodynamic

hydricity. However, this approach is fraught with computational challenges, particularly in accurately obtaining the free energy of the high charge density H^- ion, $G^o_{calc}(H^-)$. The groups of Kovács[14] and Muckerman[15] utilized the approach of Figure 5a to determine a value of $G^o_{calc}(H^-)$: the energy difference between hydride donor/acceptor pairs, $G^o([M]^{2+}) - G^o([M–H]^+)$, was computed and plotted vs. the experimental ΔG^o_{H-} value. The intercept of Figure 5a provides $G^o_{calc}(H^-)$, which can then be used in computations for hydride donors of unknown hydricity. It is worth emphasizing that although this method appears to be an "absolute" hydricity computation, because $G^o_{calc}(H^-)$ is based on experimental data there are inherent uncertainties in the absolute accuracy. Nevertheless, for solvents where many experimental hydricity values are available, the direct computation method can quite reliably predict experimental hydricity values. One drawback is that this method requires many calculations to build an appropriate training set.

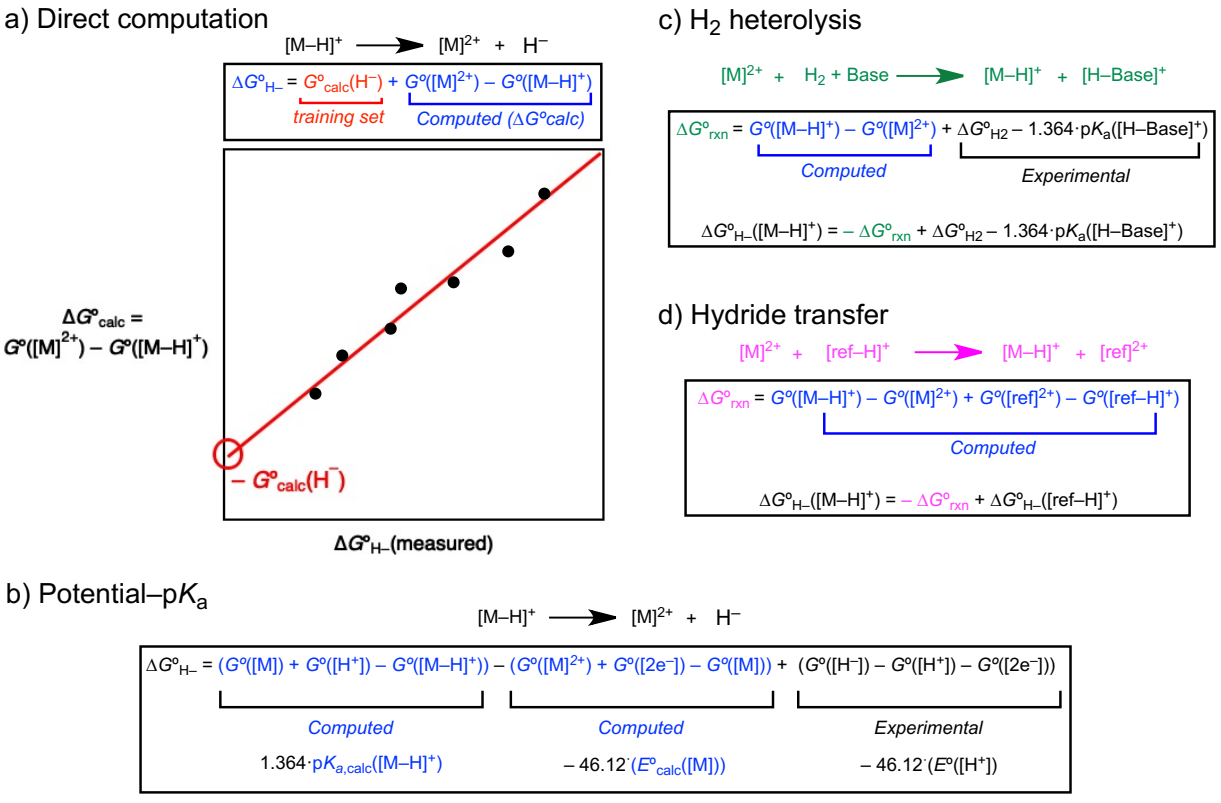

Figure 5. Computational strategy employed to estimate the energy for the hydride ion $G^o_{calc}(H^-)$ using a series of complexes with experimentally determined hydricities **(a)**. Reactions and computed parameters (blue) and experimental values (black) for potential–pK_a **(b)**, H_2 heterolysis **(c)**, and hydride equilibration **(d)** computations.

A computational version of the potential–pK_a method computes reduction potentials and acidity before employing a thermochemical cycle utilizing an experimental value for $\Delta G^{o}_{H+/H-}$ (Figure 5b).[16,17] The challenges of this method lie in finding an appropriate computational protocol that minimizes error in the determination of two distinct thermochemical values. Fortunately, there are libraries of experimental data to calibrate computational methods.

A computational approach to the "H_2 heterolysis" method (Figure 5c) calculates the energy required for heterolytic cleavage of H_2 by the metal complex of interest. Many studies utilize the H_2 cleavage approach, since the hydricity for H_2 is known in many solvents, experimental measurements are often made using H_2, and reactivity with H_2 is often a topic of interest.

Finally, there is a computational analogue to the "hydride equilibration" method (Figure 5d).[15] Such isodesmic reaction schemes, in which the type of chemical bond broken in the reactant is the same as the type of bond formed in the products, benefit from cancellation of systematic errors in the computed values, so long as the reaction partners generally have the same charge and similar size.[16,18] When calculating the hydricities for a series of related complexes, an isodesmic scheme will generally yield accurate relative hydricities that are internally consistent.

All of the computational methods described above can accurately predict thermodynamic hydricity values when performed with care. Individual instances where one method might be favored are noted above. For all of the methods, appropriate levels of theory should be selected based on a direct comparison in the system(s) of interest with experimental data, or by inspection of relevant literature studies where such comparisons were performed. Given that hydride transfer reactions inherently involve charged species, the use of continuum solvation models — and perhaps even explicit solvent molecules — is critical.[17] Including dispersion corrections may also significantly influence accuracy, particularly when ligand association/dissociation processes are involved.[19] Finally, computed hydricities should be reported with correct standard states (see above) to enable comparisons to experimental values. Computational packages typically adopt a standard state convention of 1 atm for all species, so in cases where reactants and products have different standard states a correction of –1.89 kcal/mol must be applied to bring solutes to 1 M (an additional correction is needed if solvent binds after hydride transfer, converting 1 M to neat solvent molarity).[20]

Solvent effects on thermodynamic hydricity

Surprisingly little is known about how thermodynamic hydricity changes as a function of solvent composition. The vast majority of hydricity values have been reported in acetonitrile (See spreadsheet and chart in ESI), but the new availability of thermodynamic parameters that relate H_2, H^+, and H^- in a large number of solvents (see Table 1 above)[9] has opened opportunities for new comparisons and improved understanding. Given that hydride transfer inherently involves charged species and often is followed by solvent binding to the conjugate hydride acceptor, thermodynamic hydricity is expected to change significantly based on particular solvent interactions in each medium. If the relative hydricity of two donor/conjugate acceptor pairs changes, this can lead to a change in the favorability of a reaction of interest. Therefore, tuning the medium offers opportunities to tune reactivity, as will be highlighted in a case study below.

Starting with seminal studies by Creutz and co-workers comparing the hydricities of ruthenium complexes in both acetonitrile and water,[21,22] almost all experimental knowledge of hydricity solvent dependence comes from comparisons between these two solvents (with the exception of recent studies by Yang and co-workers comparing hydricity in H_2O, MeCN, and DMSO).[8,23] Figure 6 collects transition metal hydride complexes with thermodynamic hydricity values measured in both water and acetonitrile. All metal hydride complexes studied so far are more hydridic (smaller ΔG^{o}_{H-} value) in water than in acetonitrile (although the difference is smaller than originally thought, see Figure 8). For a structurally homologous series of Cp*Ir complexes (blue circles in Figure 6b), there is a strong correlation indicating analogous trends in hydricity in the two solvents. Amongst the broader series of complexes that contain more structural diversity, the correlation is much weaker. The small molecules H_2 and HCO_2^- are significant outliers. There is a striking *compression* in the scales, with the aqueous hydricity values spanning only 20 kcal/mol while the acetonitrile values span more than 30 kcal/mol. Similar solvent-dependent behavior is observed for acidity scales.[12]

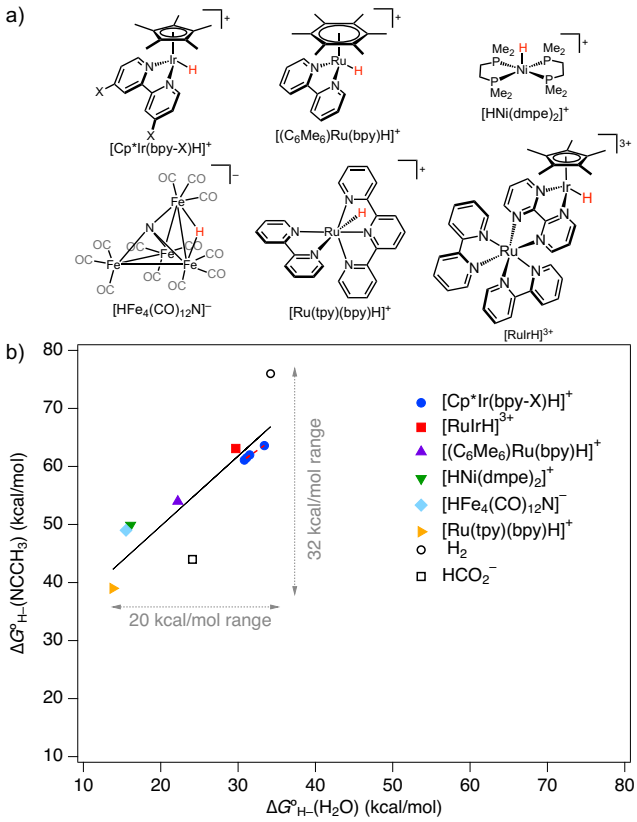

Figure 6. (a) Structures for a series of transition metal complexes with reported hydricities in both acetonitrile and water. **(b)** Aqueous hydricity values, $\Delta G^{o}_{H-}(OH_2)$, plotted versus corrected acetonitrile hydricity values, $\Delta G^{o}_{H-}(NCCH_3)$. Linear fits are provided for the full set of complexes (solid black line) as well as a family of iridium complexes (dashed red line). Adapted from reference 9.

A general model for understanding how thermodynamic hydricity changes across solvents is illustrated in Figure 7a. Building on models independently proposed by Creutz and co-workers and Goddard and co-workers,[22,24] Miller and co-workers modeled the change in hydricity moving from one solvent to another as a series of differences in transfer free energies.[9] When the hydride donor and its conjugate acceptor have similar solvent transfer free energies, the differences in hydricity will be dominated by the transfer free energy of H^- from water to organic solvents, $\Delta G^{o}_{tr}(H^-)$. As shown in Figure 7b, $\Delta G^{o}_{tr}(H^-)$ correlates well with acceptor number, suggesting that hydrides will become more hydridic (smaller ΔG^{o}_{H-} values) in solvents with higher acceptor numbers. There are many cases where the solvent transfer free energies of the hydride donor ($\Delta G^{o}_{tr}(HA^{n+})$) and acceptor ($\Delta G^{o}_{tr}(A^{(n+1)+})$) are quite different, which leads to *significant changes in the relative hydricity differences across a series of hydride complexes in different solvents*.

Additional complexity arises when the solvent ligates the conjugate hydride acceptor: while this is considered part of the normal solvation process and is roughly constant within a particular solvent, the difference in binding affinity of the two solvents must be considered when comparing hydricity values across multiple solvents.[9]

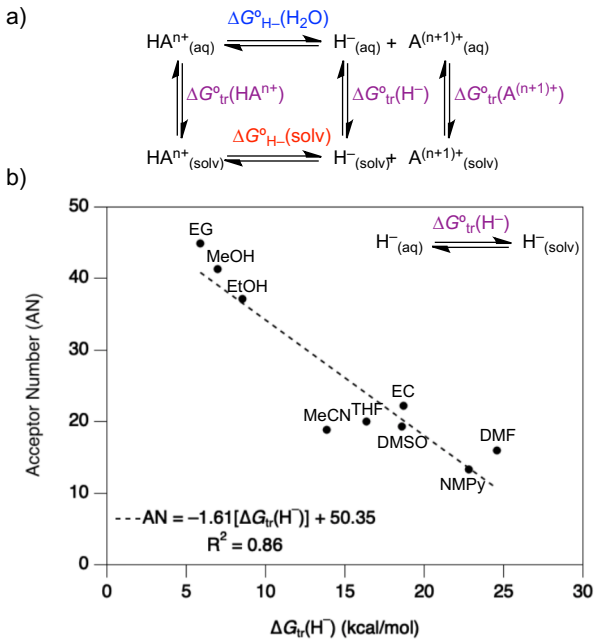

Figure 7. (a) General model for understanding how hydricity in water ($\Delta G^{o}_{H^-}(H_2O)$) differs from hydricity in organic solvent ($\Delta G^{o}_{H^-}(solv)$), based on the transfer free energy (ΔG^{o}_{tr}) of each reactant and product. **(b)** Correlation between the transfer free energy of the hydride ion from water to organic solvents, $\Delta G^{o}_{tr}(H^-)$, and the acceptor number (AN) of the organic solvent.[9] Abbreviations: ethylene gycol (EG), methanol (MeOH), ethanol (EtOH), acetonitrile (MeCN), tetrahydrofuran (THF), ethylene carbonate (EC), dimethyl sulfoxide (DMSO), N-methyl-2-pyrrolidone (NMPy), dimethylformamide (DMF). Adapted from reference 9.

The model of Figure 7a accurately predicts the solvent-dependent change in hydricity for the complexes in Figure 6 (using a combination of experimental hydricity values and computational transfer free energies).[9] This allowed the identification of two major factors that control the exact extent of change in hydricity for individual donor/conjugate acceptor pairs. First, hydride complexes with dramatic structural and charge differences exhibit the biggest differences in solvation. For example, the tricationic hydride $[RuIrH]^{3+}$ ($\Delta G^{o}_{H^-}(NCCH_3)$ = 63.1 kcal/mol) is less hydridic than $[Cp^*Ir(bpy)H]^{+}$ ($\Delta G^{o}_{H^-}(NCCH_3)$ = 62.0 kcal/mol) in acetonitrile, but $[RuIrH]^{3+}$ ($\Delta G^{o}_{H^-}(H_2O)$ = 29.7 kcal/mol) is *more* hydridic than $[Cp^*Ir(bpy)H]^{+}$ ($\Delta G^{o}_{H^-}(H_2O)$ = 31.5 kcal/mol) in water. Similarly, while $[Ru(tpy)(bpy)H]^{+}$ is 10 kcal/mol more hydridic than $[HFe_4N(CO)_{12}]^{-}$ in acetonitrile, it is less than 2 kcal/mol more hydridic in water. The differences

in charge, nuclearity, and supporting ligands that affect solvation of each species are likely responsible for the observed changes. Furthermore, as the number of reported hydricity values increases, it will be easier to identify outliers that may be worth reevaluating.

Second, striking differences are observed when either the hydride donor or acceptor is a gas. Few transition metals will fulfill this criterion, but many small molecules do. This is significant because the choice of standard states means that solvation of gases is not considered. These small molecules thus change as a function of solvent in ways that are distinct from the metal hydride complexes. For example, CO_2 is a gaseous hydride acceptor, and its hydricity is almost unchanged moving between water and acetonitrile. This has been exploited in catalyst development, where hydride transfer to CO_2 may be unfavorable in one solvent, but favorable in another, as expanded on below.

What can be Learned from Thermodynamic Hydricity

Knowledge of thermodynamic hydricity values provides insight into experimental observations and enables predictions of new reactivity. Number line representations provide an intuitive method of comparing hydricity between different hydride donor/acceptor pairs. Figure 8 presents a selection of hydricity values for various transition metal and organic hydride donors in water, acetonitrile, dimethyl sulfoxide, and tetrahydrofuran. A hydride that appears farther to the right on the number line (smaller ΔG^{o}_{H-} value) is more hydridic; when comparing two hydride donor/conjugate acceptor pairs, the hydride of the pair that appears farther to the right will be thermodynamically favored to transfer H^- to the acceptor of the other pair (with the magnitude of favorability reflected in the span between the two pairs). A complete table of hydricity values of transition metal hydrides, which includes additional entries beyond the comprehensive table published in 2016, is included as ESI. To enable comparisons across solvents, the hydricity values in acetonitrile and dimethyl sulfoxide are shifted on the number line by 13.75 and 12.6 kcal/mol, respectively. As discussed above, this corrects systematic differences in scales by using the same aqueous ΔG^{o}_{H2} value (based on $E^{o}_{H\bullet/H-} = 0.81$ V) to derive all scales. As introduced above, hydride donors are somewhat more hydridic (smaller ΔG^{o}_{H-} values) in water than MeCN, and Figure 8 illustrates how H_2 and HCO_2^- have distinct variations across solvents. The most prominent solvent effects are cases where the relative hydricity (which is unaffected by the correction factors applied in Figure 8) changes between solvents, as seen for $[HNi(TMEPE)_2]^+$ and HCO_2^- in dimethyl

sulfoxide/acetonitrile/water. To illustrate how knowledge of thermodynamic hydricity guides catalyst development, two case studies are presented. In each, the thermodynamics of hydride transfer from a metal hydride to CO_2 are adjusted, either by tuning catalyst structure or by changing the solvent.

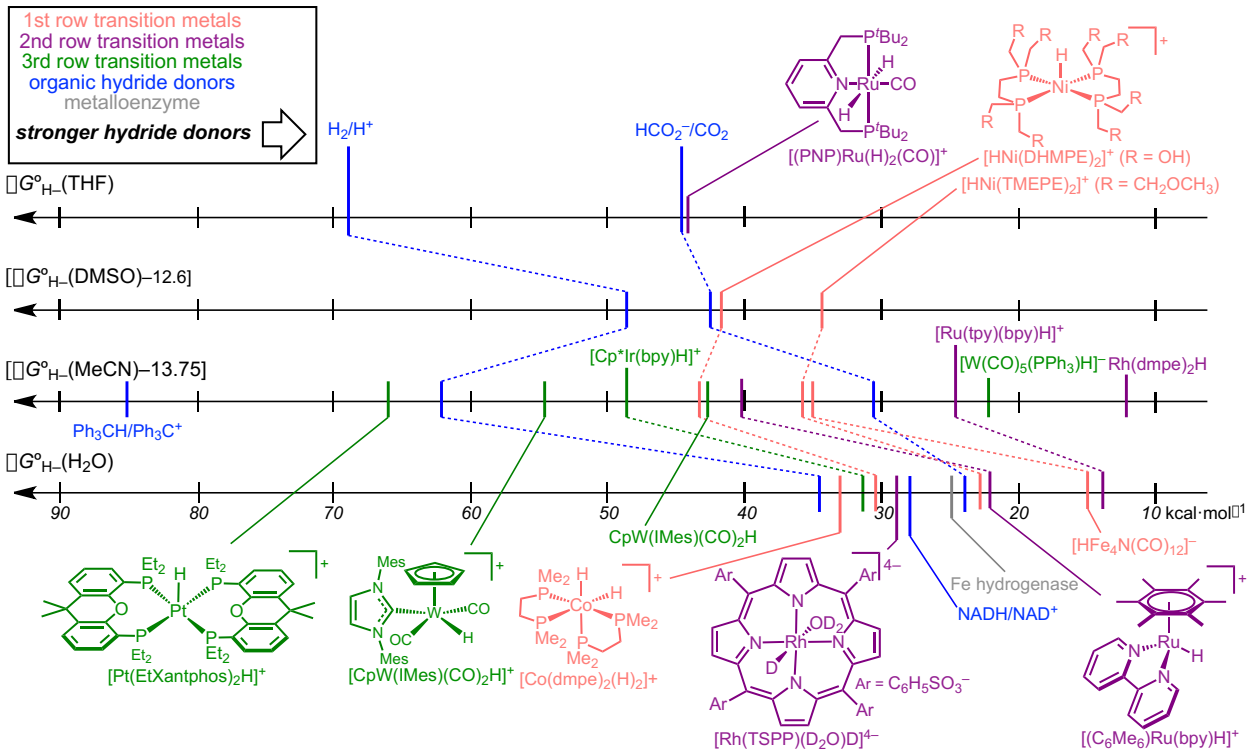

Figure 8. Comparing thermodynamic hydricity values of selected transition-metal-, organic-, and enzyme-based hydride donors in water (H_2O), acetonitrile (MeCN), dimethyl sulfoxide (DMSO), and tetrahydrofuran (THF). As a result of differences in convention for the construction of scales, correction factors of 12.6 (DMSO) and 13.75 (MeCN) are applied to provide accurate comparisons of how hydricity changes across solvents. Within any given solvent, the relative values are not affected by the correction factors. See ESI for a complete table of hydricity values.

Ceballos and Yang introduced a strategy that considers the relationships between ΔG^{o}_{H-} and pK_a to identify conditions where CO_2 reduction to formate is thermodynamically favored over proton reduction to H_2 (Figure 9). In the green region of Figure 9, the metal hydride is hydridic enough to react with an acid of given pK_a to produce H_2; in the blue region, H_2 evolution is endergonic. In the region where the acid has a pK_a value above ca. 25 and the metal hydride is hydridic enough to react with CO_2 to produce formate, thermodynamic selectivity for formate over H_2 is possible.[25] This approach guided the choice of $[Pt(dmpe)_2][PF_6]_2$ for electrocatalytic CO_2 reduction in acetonitrile. The hydride $[HPt(dmpe)_2][PF_6]$ undergoes favorable hydride transfer to

CO_2 (ΔG^o = –2.2 kcal/mol, a value independent of acid pK_a) and has a pK_a amenable to the use of weak acids (Figure 10 in blue). Phenol, in particular, has an appropriate pK_a to protonate $Pt(dmpe)_2$ and generate the hydride $[HPt(dmpe)_2][PF_6]$, but further protonation of $[HPt(dmpe)_2][PF_6]$ with phenol to generate H_2 is unfavorable. This scenario enabled the selective generation of formate (>90% Faradaic efficiency, FE) at 90 mV overpotential in acetonitrile.[25,26]

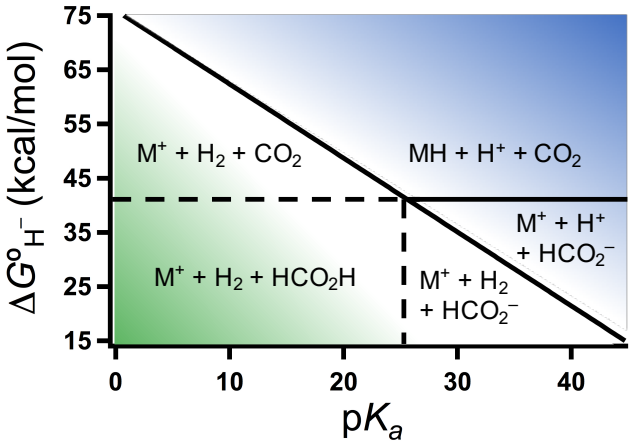

Figure 9. Regions of predicted metal hydride reactivity with CO_2 and H^+ as a function of ΔG^o_{H-} and pK_a. Adapted from reference 25.

The complex $[HPt(depe)_2]^+$ is slightly less hydridic than the dmpe analogue, such that the hydride transfer reaction with CO_2 forms an equilibrium mixture in acetonitrile ($\Delta G^o \sim 0$ kcal/mol, Figure 10 in green). This isoergic situation raised the prospect of *reversible* CO_2/HCO_2^- electrocatalysis. An appropriate acid/base pair was chosen to match the pK_a value of $[HPt(depe)_2]^+$ (pK_a = 29.7 in MeCN), such that both hydride transfers and proton transfers would be isoergic. This catalyst system is capable of formate oxidation at –1.4 V vs $Cp_2Fe^{+/0}$ (TOF < 0.5 s^{-1}; FE = 90%) and CO_2 reduction at –2.0 V vs $Cp_2Fe^{+/0}$ (TOF < 0.5 s^{-1}; FE = 97%). The overpotential for CO_2 reduction of 48 mV was consistent with access to reversible catalysis.[27] These studies illustrate how a thorough understanding of thermodynamic parameters, particularly hydricity, can guide the selection of catalysts and conditions for selective and/or reversible CO_2 reduction.

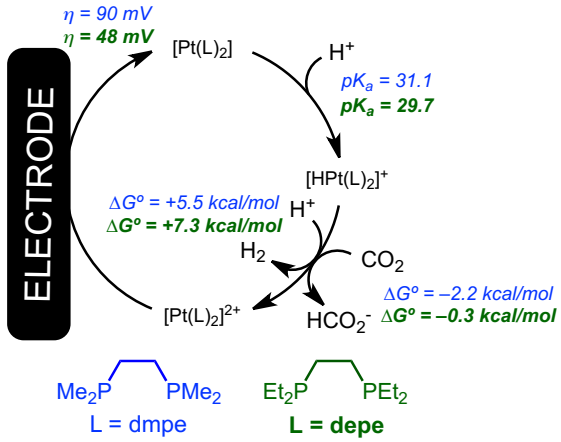

Figure 10. Catalytic cycles for the electrocatalytic reduction of CO_2 in acetonitrile by two Pt complexes, $[HPt(dmpe)_2]^+$ (blue) and $[HPt(depe)_2]^+$ (green), highlighting the thermodynamic values associated with each step in the cycle.

The developing understanding of the influence of solvation on thermodynamic hydricity led to a new method for controlling catalytic pathways: rather than making structural changes to the catalyst itself, the solvation environment can be modified (Figure 11). A study by Wiedner and co-workers elegantly demonstrates how differences in the thermodynamic hydricity of $[(H)_2Co(dmpe)_2]^+$ in THF and water impact CO_2 reduction.[28] CO_2 hydrogenation by $HCo(dmpe)_2$ was first studied in THF. Hydride transfer from the monohydride to CO_2, which was predicted to be exergonic ($\Delta G^o = -8$ kcal/mol), produced $[Co(dmpe)_2]^+$, which in turn activated H_2 to produce the dihydride, $[(H)_2Co(dmpe)_2]^+$. Hydride transfer from $[(H)_2Co(dmpe)_2]^+$ was predicted to be endergonic by 10 kcal/mol, however, and reactivity was dependent on the use of Verkade's base to deprotonate the weakly acidic dihydride complex and regenerate $HCo(dmpe)_2$. Under these strongly basic THF conditions, $HCo(dmpe)_2$ is an excellent CO_2 hydrogenation catalyst, TOF = 3400 h^{-1} at 21 ºC and 1 atm of H_2/CO_2.[29]

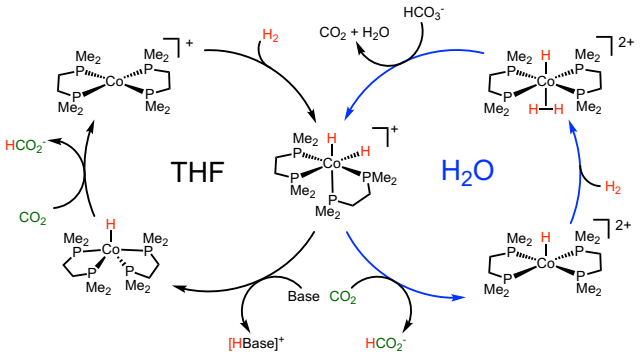

Figure 11. Catalytic reduction of CO_2 by $[(H)_2Co(dmpe)_2]^+$ in THF and H_2O. Hydride transfer occurs from $HCo(dmpe)_2$ in THF, but from $[(H)_2Co(dmpe)_2]^+$ in water, due to solvent effects on hydricity.

As discussed above, the hydricity of formate does not change dramatically in organic solvents compared to water, while many metal hydride complexes are more hydridic in water (Figure 8 above). Taking advantage of this trend, Wiedner and co-workers found that $[(H)_2Co(dmpe)_2]^+$ is sufficiently hydridic in water to reduce CO_2 to formate directly. This represents a change in the free energy of reaction of more than 10 kcal/mol simply by changing the solvent. As a result, $[(H)_2Co(dmpe)_2]^+$ was able to catalyze CO_2 hydrogenation without strong base, in aqueous carbonate solutions at room temperature (TOF = 560 h^{-1} at 100 ºC and 34 atm of H_2/CO_2).

Outlook and Challenges

Thermodynamic hydricity is now used routinely by many groups to characterize transition metal hydride complexes and predict hydride transfer reactivity. Sharing insights into the various experimental and computational methods will hopefully inspire more researchers to determine the hydricity of new molecules. Looking ahead, there is a clear opportunity to expand the scope of solvents for which hydricity scales have been developed. Each hydricity measurement in solvents other than acetonitrile will fill in new details. Several examples have demonstrated that solvent-dependent hydricity can be leveraged to adjust the favorability of CO_2 reduction to formate. This approach should also be applicable to other hydride transfer reactions, and interesting opportunities remain unexplored in these areas. One challenge facing further development is the lack of hydricity values available for simple organic compounds. Ubiquitous substrates in hydride transfer catalysis,

such as ketones and aldehydes, do not have experimental hydricity values for the conjugate hydride donor, to our knowledge.

III. Kinetic Hydricity

Introduction

Understanding the kinetic hydricity (the rate at which a hydride is transferred) of a transition metal hydride is important because hydride transfer is a common elementary step in a plethora of catalytic (de)hydrogenative reactions. Unfortunately, despite the importance of kinetic hydricity, it is often difficult to determine experimentally. This is in part due to the fact that kinetic hydricity measurements are highly dependent on a variety of different factors, including the identity of the solvent and the choice of hydride acceptor.[5] A further complication is that unless the hydride transfer occurs in a single elementary step, it can be difficult (if not impossible) to determine the elementary rate constant associated with hydride transfer. Nevertheless, comparisons of kinetic hydricity under the same conditions have provided, and will continue to provide, valuable fundamental understanding of the reactivity of transition metal hydrides. This section is structured in an analogous fashion to Section II and provides a tutorial on best methods for determining kinetic hydricity as well as our opinions on current challenges and future research directions.

Experimental considerations for determining kinetic hydricity

Multiple factors must be considered in the design and execution of kinetic hydricity measurements. Some of these are relevant to any kinetic study, whereas others, such as choosing a hydride acceptor, are specific to the determination of kinetic hydricity. Initially, a researcher interested in measuring kinetic hydricity needs to assess whether a reaction is suitable for kinetic studies. To accurately perform kinetics experiments, it is essential to identify all of the products from the hydride transfer reaction. Additionally, it must be possible to monitor the concentration of either the reagents or the products (preferably both) as a function of time, so the spectroscopic characteristics of the species present in solution is crucial. For instance, if a transition metal hydride is paramagnetic, it is likely not possible to measure the rate of hydride transfer using ^{1}H NMR spectroscopy, but the presence of a carbonyl ligand or the M–H bond itself (if it has an intense stretch), may enable the reaction to be monitored using infrared (IR) spectroscopy.

Alternatively, the lack of characteristic IR absorptions in a diamagnetic complex that remains colorless throughout a reaction may mean that the reaction is best monitored using NMR spectroscopy, but only if the reaction occurs slowly enough to do so.

A major difference between measuring kinetic and thermodynamic hydricities is that kinetic measurements require the timescale of the spectroscopic method to match the rate of the hydride transfer reaction. Additionally, the spectroscopic method must be sensitive enough to detect the changes in concentration that occur as a function of time during hydride transfer. Table 2 contains information on the sensitivity and timescale of several common spectroscopic methods that can be used to measure kinetic hydricity.

Table 2. Sensitivity and Timescale Approximations for Common Spectroscopic Techniques Used to Measure Kinetic Hydricity.

Measurement Method	Sensitivity (Concentration Range)	Timescale of Reaction ($t_{1/2}$)
^{1}H NMR[a]	>5 mM	> 1 minute[d]
^{31}P NMR[a]	>10 mM	> 5 minutes[d]
IR[b]	~20 mM	> 10 seconds[d]
UV-Vis[b]	~0.01-1 mM[c]	> 10 seconds
Stopped-Flow (UV-Vis)	~0.01-1 mM[c]	> 500 ms
Transient Absorption (UV-Vis)	~0.01-1 mM[c]	> 10 ns

[a]Assumes the use of a 400 MHz field strength and a 5 mm tube. Access to instruments with higher field strength, larger tube diameters, or the use of a cryoprobe can greatly enhance sensitivity. [b]Assumes a path length of 2 mm for an IR solution cell and 1 cm for a UV-Vis observation cell. Observation cells with longer path lengths can greatly enhance the sensitivity of these measurements. [c]Concentration of experiment depends upon the molar absorptivity of either of the reactants. [d]For these methods, the sensitivity can be easily improved by increasing the number of scans taken of the sample for each data point. However, this will increase the timescale of the reaction that can be measured and caution should be taken when applying this method to increase sensitivity.

Many kinetic measurements are made using ultraviolet-visible (UV-Vis) absorption spectroscopy, which offers high sensitivity, excellent time resolution, and the ability to accurately determine kinetic profiles. Additionally, in the case of hydride transfer to triphenylmethyl cation (trityl), the disappearance of the trityl cation can be monitored readily as it absorbs in the visible light range (λ_{max} = 430 nm, $\varepsilon = 3.2 \times 10^4$ M^{-1} cm^{-1}).[30] However, UV-Vis spectra can be complicated to interpret if one or more intermediates are present during the experiment and it can be difficult to assess if there is clean conversion from the reactants to the products. In contrast, NMR spectroscopy provides a wealth of chemical information. The diagnostic upfield resonances

characteristic of diamagnetic transition metal hydrides are convenient for reaction progress monitoring because they rarely overlap with other signals. Nevertheless, NMR spectroscopy generally suffers from low sensitivity, although the intensity of signals belonging to hydride complexes can sometimes be enhanced by polarization techniques (*para*-hydrogen induced polarization, PHIP, or dynamic nuclear polarization, DNP).[31] The timescale for NMR spectroscopy is also relatively slow, such that many hydride transfer reactions are too fast to be monitored. IR spectroscopy offers both good time resolution and a large amount of chemical information when characteristic absorptions, such as CO or M–H stretches, are present. Challenges with this method include IR absorption by the solvent, which can restrict the solvent choice to those with few vibrational normal modes; alternatively, isotopically-labelled solvents can shift solvent vibrations out of the spectral region of interest.

Stopped-flow instruments equipped with either an UV-Vis or IR detector enable monitoring of rapid reactions. For example, reactions that finish within ~1 second of mixing are easily examined using stopped-flow techniques because the reagents are combined by the instrument and injection timing is synchronized with acquisition. In stopped-flow experiments, solutions of hydride donor and reference acceptor are prepared independently. The solutions are then simultaneously injected and mixed in the instrument immediately prior to spectral acquisition; delay times between mixing and the first spectrum are on the order of milliseconds. Unlike NMR spectroscopy, which requires locking and shimming before acquisition, UV-Vis and IR do not require any adjustments before spectral acquisition. The power of stopped-flow with UV-Vis detection is highlighted by Bullock and co-workers in hydride transfers to trityl cation[30,32,33] (Figure 12a); several groups have used similar methods to measure the rates of hydride transfer to CO_2 (Figure 12b).[34,35] In general, stopped-flow techniques are particularly valuable for kinetic hydricity determination relative to other techniques because many hydride transfer reactions are too rapid to measure using traditional techniques. However, stopped-flow instruments are not always accessible, limiting their widespread adoption. Further, some hydride transfer reactions are too fast to monitor even using stopped-flow and the use of techniques with even better time resolution, such as transient absorption spectroscopy, will be required to monitor reaction kinetics. Nevertheless, to date, there are no examples of the measurement of kinetic hydricity using transient absorption spectroscopy, likely because of the specialized equipment required and the problems

with initiating the reaction. The measurement of rates for extremely rapid hydride transfer reactions remains a challenge for the field.

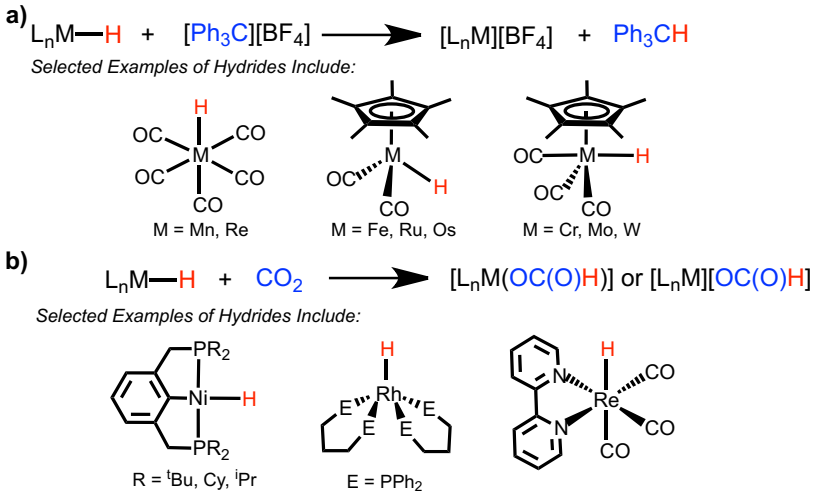

Figure 12. Examples of transition metal hydrides for which a stopped-flow instrument has been used to measure kinetic hydricity using **(a)** trityl cation and **(b)** CO_2 as the acceptor.

The selection of a hydride acceptor is a key feature in determining kinetic hydricity, as the choice of acceptor can dramatically alter the rates of hydride transfer and it may be possible to measure the kinetic hydricity with one acceptor but not with another (Table 3). To date, kinetic hydricity studies with transition metal hydrides, which have primarily been performed in organic solvents, have focused on four categories of acceptors: (1) Trityl cation has tunable thermodynamics for hydride transfer via substitution of the phenyl groups and has been used in many previous studies on kinetic hydricity, allowing for direct comparisons; (2) NAD^+ (nicotinamide adenine dinucleotide) mimics consisting of substituted pyridinium cations, which allow for tuning of the acceptor and may be relevant to select catalytic reactions; (3) Carbon dioxide, which is a substrate of intense interest for catalytic applications but cannot be tuned; (4) Protonated ketones and imines, which also allow for tuning of the acceptor and are directly relevant to ionic and step-wise hydrogenation reactions. Unfortunately, experimental thermodynamic hydricities are not yet available for the C_α–H bond of alcohols and amines, and although some computational values have been reported,[15,36] confirming these values experimentally will be of value to the community.

Table 3. Thermodynamic hydricity values of common hydride acceptors in acetonitrile.

Hydride Acceptor	ΔG^{o}_{H-} of Conjugate Hydride Donor (kcal/mol)	Reference	Typical Observed Rate Constants (k_{obs}, M^{-1} s^{-1})[a]
	Triarylmethane Cations		$0.1–10^6$
	$[Ar_3C^+] \xrightarrow{[H^-]} Ar_3CH$		
Ar = 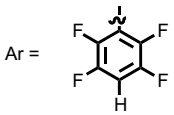	116	3	
Ar = 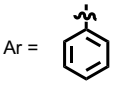	96–99	3	
Ar = 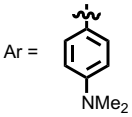	74–76	3	
	NAD^+ Mimics		$10^{-3}–10^3$
	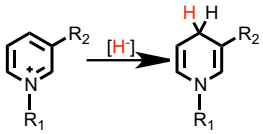		
$BNAP^+$ 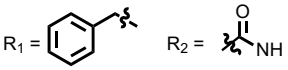	59	37	
NMP^+ $R_1 = R_2 = Me$	41	22	
	CO_2		$10^{-4}–10^2$
	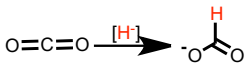		
CO_2	44	2,22	

[a]Second order rate constants for hydride transfer to the given class of substrates. The values reported here are the range of rate constants reported in refs. 30, 32, 33, and 38 for trityl cation measured mostly in CH2Cl2; refs. 15, 21 and the references therein for NADH mimics measured in a variety of solvents); and ref. 34 and the references therein for CO2 measured in a variety of solvents.

The choice of hydride acceptor initially needs to be governed by thermodynamics, as a hydride donor may not react with an acceptor whose conjugate hydride donor has a smaller ΔG^{o}_{H-} value. If the reaction is only slightly endergonic (*ca.* 2 kcal/mol or less) the kinetics of approaching equilibrium may be observable, but it is easier to study reactions which are thermodynamically favorable. In this regard, trityl cation is often an ideal hydride acceptor as it can be used with many transition metal hydrides, even those that are weakly hydridic (large ΔG^{o}_{H-} value), due the fact that triphenylmethane is an extremely weak hydride donor (ΔG^{o}_{H-} 96–99 kcal/mol in acetonitrile).[3] Additionally, substituted triarylmethanes have hydricity values between 74 and 116 kcal/mol in acetonitrile, so the triarylmethyl scaffold is highly tunable.[3] A major benefit of using 1,4-dihydropyridine and derivatives as the hydride acceptor is that ΔG^{o}_{H-} can be tuned without changing its fundamental reactivity. Specifically, substituted dihydropyridines have ΔG^{o}_{H-} ranging from 57–68 kcal/mol in acetonitrile,[3] with NADH mimics having hydricities as low as 41 kcal/mol.[22] In contrast, it is not possible to tune CO_2 (ΔG^{o}_{H-} = 44 kcal/mol in acetonitrile), which means that only strong hydride donors are compatible with the use of CO_2 as an acceptor.

The selection of solvent is another critical factor in determining kinetic hydricity. Firstly, in order to make high quality kinetic measurements, the reactants should be stable and soluble in the selected solvent. Researchers should also be aware that solvent binding to coordinatively unsaturated metal complexes can affect the thermodynamics of hydride transfer, and as such the values in Table 3 may not be directly applicable to a given transfer. As well as affecting ground state properties, the solvent may also directly impact a transition state (*vide infra*). As a result, comparison of the kinetic hydricity of two different compounds in two different solvents should only be made with great care. Further, the products of a reaction may change when the solvent is varied, so it is important to ascertain that changing the solvent does not to alter the reaction.

Experiments that provide context about kinetic hydricity

Once it has been determined that kinetic hydricity measurements can be made for a particular choice of transition metal hydride and acceptor, there are several experiments that can provide useful information about the mechanism of hydride transfer. These include measuring kinetic isotope effects, studying the effects of temperature on the kinetic hydricity, and probing the effects of changes to the ligands on kinetic hydricity.

The synthesis of transition metal deuterides allows for the measurement of kinetic isotope effects (KIEs) associated with hydride transfer reactions, which provides information about the structure of the transition state. Given that D_2 and deuterated hydride sources such as $NaBD_4$ are readily available, it is typically not difficult to synthesize metal deuterides. The magnitude and direction (where direction is either normal or inverse, greater or less than 1) of the KIE is expected to be dependent on the differences in bond zero-point energies (ZPEs).[39] In a notable example of how KIEs can be used to gain information about the structure of a transition state, Bullock and co-workers used KIEs to provide evidence for a nonlinear M–H–C angle in the transition state of hydride transfer from a tungsten hydride to a trityl cation (Figure 13).[38] To perform their analysis they compared the measured KIE with the theoretical maximum classical isotope effect, as maximum isotope effects occur in symmetric, linear transition states. In the case of a transition state structure with linear, symmetric hydride transfer (where the M–H–C bond angle equals 180°), the measured KIE should match the maximum isotope effect predicted by classical models (excluding tunneling) (Figure 13a). If the structure deviates from linear (M–H–C <180°), the KIE will be reduced. As Bullock and co-workers measured a KIE of 1.8, which is significantly less than the theoretical maximum KIE (3.5), they concluded that hydride transfer likely occurs via a nonlinear transition state.

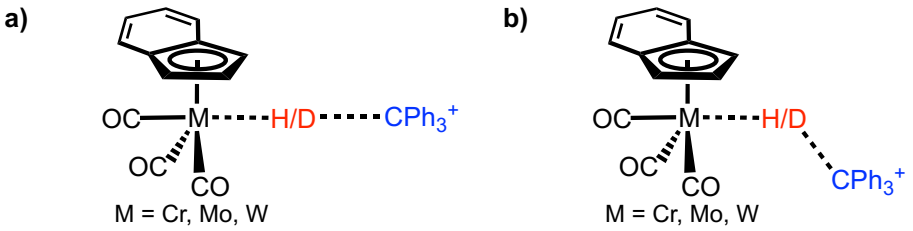

Structure Leading to Maximum KIE

Figure 13. Examples of transition state structures for hydride or deuteride transfer to trityl cation that would lead to a **(a)** maximum theoretical KIE and **(b)** KIE less than the theoretical maximum.

For CO_2 insertions into metal hydrides, inverse KIEs are often observed because in the rate-determining transition state C–H bond formation is nearly complete and the M–H bond is essentially fully broken. As a result, the ZPE differences are larger for the deuterated system compared to the protio system because the gap between the vibrational energy levels is greater for the C–H bond compared to the M–H bond. In more complicated scenarios, KIEs (and in particular the temperature-dependence of a KIE) can support a hypothesis of tunneling being involved in the

hydride transfer transition state.[5] The study and interpretations of KIEs, however, is complicated by the presence of potential equilibrium isotope effects[40] and in the case of transition metal hydrides exchange between proton sources in the solvent and metal deuterides, which can occur even if only trace amounts of H_2O are present. Additionally, the assumption that KIEs are dominated by differences in ZPE terms is not always valid, particularly for transition metal complexes.[41] As such, researchers are encouraged to read further about the subject in order to gain a comprehensive understanding of KIEs in hydride transfer reactions before attempting to interpret experimental results.

The effects of temperature on the rate constant of hydride transfer can be used to obtain the activation parameters for a reaction. If the reaction being monitored is an elementary step, or if elementary rate constants can be elucidated, an Eyring plot can provide both the enthalpy ($\Delta H^{\ddagger}$) and entropy ($\Delta S^{\ddagger}$) of activation. Alternatively, numerical modelling computer programs are capable of simulating concentration profiles from kinetics reactions directly and in this case $\Delta H^{\ddagger}$ and $\Delta S^{\ddagger}$ can be obtained without the approximations inherent to linearization of the Eyring equation. Activation parameters provide understanding about the nature of transition states for hydride transfer. For example, the barrier for CO_2 insertion into $[Ru(tpy)(bpy)H]^+$ in isopropanol is lowered by 3.9 kcal/mol at 298 K when the cationic Lewis acid $LiNTf_2$ (NTf_2 = bis(trifluoromethane)sulfonamide) is present, but this value by itself provides no information about why the barrier is lower.[34] The activation parameters indicate that there is only a small difference in $\Delta H^{\ddagger}$ (9.1 ± 0.3 kcal/mol with no Lewis acid and 10.2 ± 0.3 kcal/mol with $LiNTf_2$) and a much larger difference in $\Delta S^{\ddagger}$ (–33 ± 2 cal/mol K with no Lewis acid and –16 ± 2 cal/mol K with $LiNTf_2$) when the Lewis acid is present. This indicates that the transition state for CO_2 insertion is less ordered in the presence of $LiNTf_2$, likely because a solvent molecule that is initially bound to Li^+ is released when Li^+ stabilizes the transition state for hydride transfer. In the case of a complicated reaction mechanism where the elementary steps cannot be distinguished, it is still possible to obtain information about activation parameters via the Arrhenius equation. The Arrhenius equation can be valuable because, in contrast to the Eyring equation, the dependence of $\ln(k)$ on T^{-1} should remain linear over a large range of temperatures as E_a continues to depend linearly on T^{-1}.

Kinetic hydricity measurements that result in a single second-order rate constant provide limited information. Instead, a series of measurements of kinetic hydricity where only one variable, such as the ancillary ligand or solvent, is changed provides more context. Varying the ancillary

ligand can be useful for understanding the nature of hydride transfer and can aid in the rational design of catalysts. Currently, however, there are relatively few detailed studies examining ligand effects on hydride transfer in a systematic manner.

In general, electron-rich ligands appear to increase the kinetic hydricity of a transition metal hydride. This has been demonstrated in results showing that as the ancillary ligand becomes more electron rich, the rates of CO_2 insertion into a metal hydride increase.[35] For example, Sullivan and Meyer showed that the rate of CO_2 insertion into *fac*-Re(4,4'-X-bpy)$(CO)_3$H increases as the bpy ligand becomes more donating (Figure 14).[42] These data were used to support a transition state with a large degree of charge separation. There is also a relative paucity of information on steric effects in kinetic hydricity, although results showing that the steric properties of the ancillary ligand influence the rate of hydride transfer from (^{R}PCP)NiH (where ^{R}PCP = 2,6-$C_6H_3(CH_2PR_2)_2$ and R = ^{t}Bu, Cy, ^{i}Pr) to CO_2, suggest that even when a hydride acceptor as small as CO_2 is utilized, steric effects matter (Figure 15).[35] Nevertheless, the development of more structure-activity relationships exploring the effect of the ancillary ligand on kinetic hydricity would undoubtedly be valuable to the community.

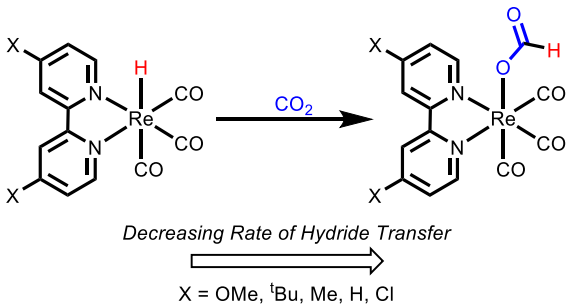

Figure 14. Substituted bipyridine complexes used to determine the ligand electronic effect on CO_2 insertion by Sullivan and Meyer.[42]

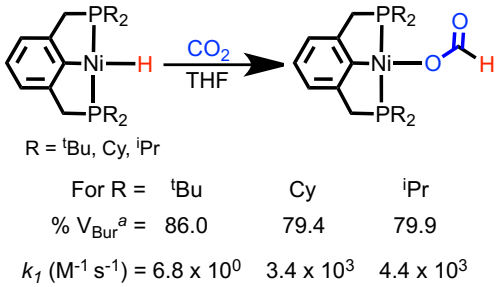

Figure 15. Nickel pincer complexes for the elucidation of steric effects on the kinetics of hydride transfer to CO_2. [a]The value of $\%V_{Bur}$ is the percent buried volume as calculated by the computer program Samb*V*ca as a measure of the occupied space (steric congestion) about the metal atom. For these calculations, the parameters used included a 3.5 Å sphere centered at the Ni atom, bond

radii scaled by 1.17, and hydrogen atoms were included in the calculation. Data taken from Table 2 of ref. 35.

Bullock and co-workers and Bruno and co-workers independently took an alternative approach in which they varied the hydride acceptor and studied hydride transfer from tungsten and molybdenum hydrides to different *para*-methoxy substituted trityl cations.[32,43] Specifically, Bullock and co-workers reported that the observed rate constants for hydride transfer from $Cp^*(CO)_3MoH$ to $Ph_n(p\text{-}MeOC_6H_4)_{3-n}C^+BF_4^-$ (n = 3, 2, 1, 0) ranged from 1.4 M^{-1} s^{-1} to 6.5 x 10^3 M^{-1} s^{-1} for n = 0 and n = 3, respectively, indicating a lowering of kinetic hydricity when the acceptor is more electron rich (Figure 16). The change in the kinetic isotope effects between these reactions was negligible, consistent with all of them proceeding via the same mechanism.[38] Nevertheless, this study highlights a limitation of current investigations exploring kinetic hydricity, which have not looked at correlations in the rate of hydride transfer across different classes of acceptors. For example, is there a correlation in the rates at which a series of transition metal hydrides transfer a hydride to CO_2 or NAD^+? As a result, the applicability of data collected with one acceptor to hydride transfer with a different acceptor is unknown.

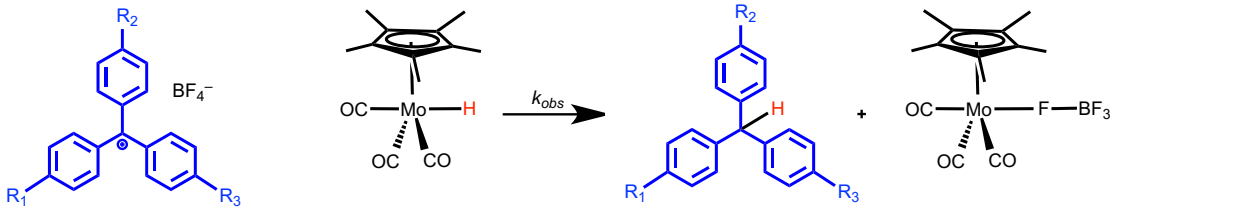

Figure 16. Rate constants for the reaction of $Cp^*Mo(CO)_3H$ with mono-, di-, tri-, and unsubstituted trityl cation. Data taken from Table 2 of ref. 38.

Solvent effects on kinetic hydricity

Information about how solvent impacts kinetic hydricity provides context about the relative rates of hydride transfer and can be used to make inferences about the reaction mechanism. In turn, this information can be used to tune a catalytic system to either promote or inhibit hydride transfer. The solvent in which hydride transfer occurs can impact the transition state in several ways. In some cases, solvent can stabilize a transition state through hydrogen bonding, which is directly related to the molecular structure of the solvent. In other cases, a more general property of the

solvent is responsible for modifications in the rate. For example, several hydride transfer studies to trityl cation and CO_2 have demonstrated a dependence of the rate on solvent polarity.[30,43,44] In the case of hydride transfer to trityl cation, Sarker and Bruno compared the rate of hydride transfer for a series of CpM and Cp*M hydride complexes (M = Mo and W) in acetonitrile to the data collected by Bullock and co-workers in dichloromethane.[30,43] They found that, in general, hydride transfers occurred more quickly in acetonitrile than in dichloromethane. This observation was attributed to a reduction in ion-pairing effects in acetonitrile, which facilitated faster reactions.

Quantitative comparisons of the effect of solvent on hydride transfer from a metal to CO_2 (CO_2 insertion) have been made by several groups. Typically, the dielectric constant (ε), acceptor number (AN), and/or the Dimroth-Reichart parameter for photoelectronic excitation (ET_{30}) are used as measures of solvent properties.[45] As a case study, we can consider the data reported by Ishitani and co-workers for CO_2 insertion into [Ru(tpy)(bpy)H][PF_6] (Figure 17a).[44] The data for hydride transfer to CO_2 correlate poorly to ε, probably due to the fact that the constant considers the solvent as a continuum, rather than composed of discrete molecules (Figure 17b). In contrast, AN correlates relatively well with the rates of CO_2 insertion (Figure 17c). This is likely because AN is a measure of the Lewis acidity of a solvent based on discrete molecular interactions, and as a result AN provides general information on stabilizing interactions between a solvent and a Lewis basic transition state. ET_{30} can account for similar stabilizing interactions of solvent and solute for charge separation, as it is defined as the energy of a $\pi \rightarrow \pi^*$ absorption for a solvatochromic pyridinium-*N*-phenolate betaine dye. For this dataset, ET_{30} gives a better correlation than AN, likely due to subtle differences in how the parameter accounts for discrete molecular interactions such as hydrogen bonding. (Figure 17d). Regardless of the quantifying solvent parameter that provides the best fit, the dependence of kinetic hydricity on solvent can provide important insight into the transition state of hydride transfer, with parameters that model the solvent as a continuum (for example ε) indicating a build-up of localized charge, and parameters such as AN or ET_{30} indicating a role for specific solvent interactions with the transition state.[46]

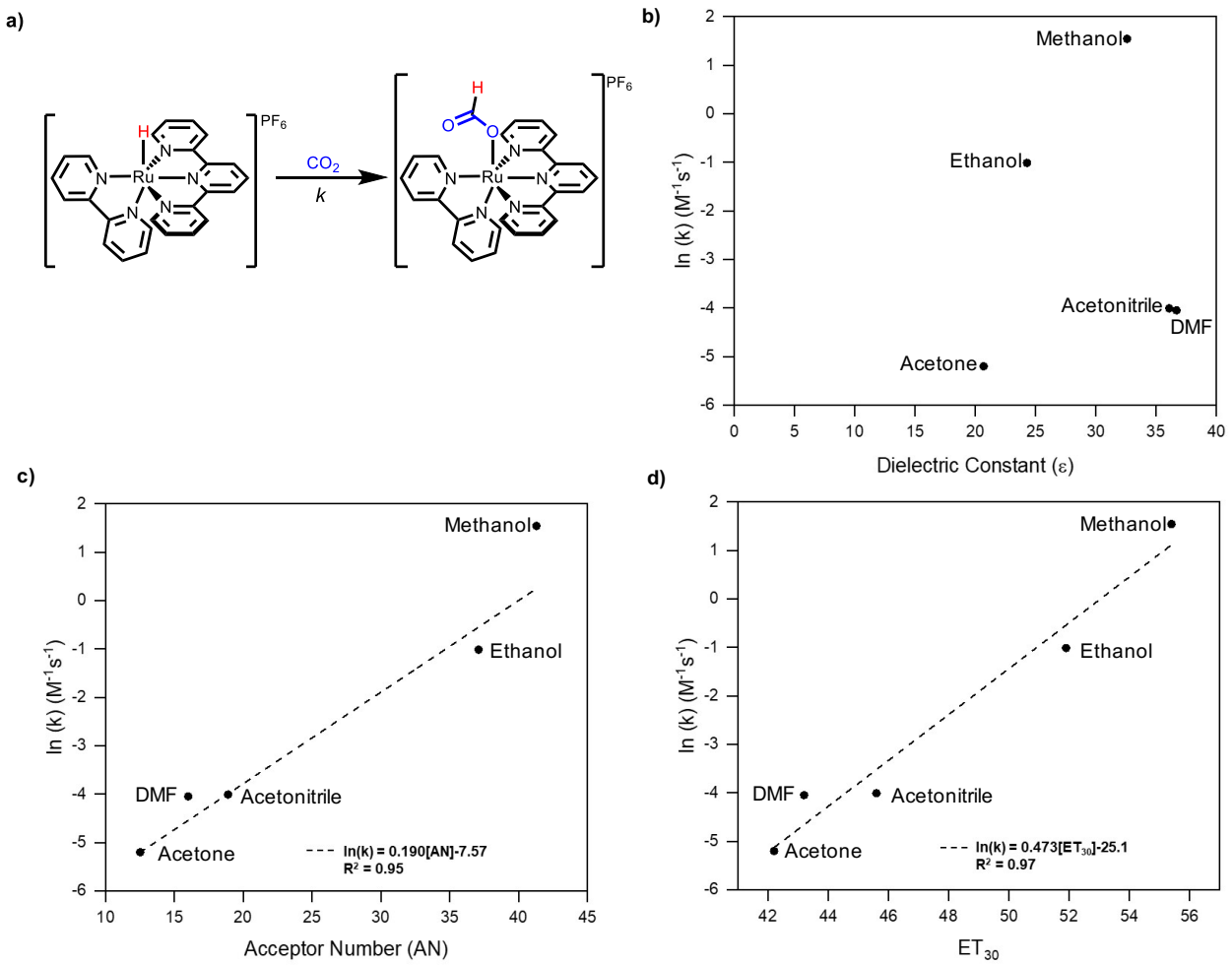

Figure 17. (a) Model complex for determining solvent effects for outer-sphere CO_2 insertion. Graphs of rate constant for CO_2 insertion (k) vs. **(b)** dielectric constant (ε); **(c)** AN; **(d)** ET_{30}. Data taken from Table 3 of ref. 44.

Computational methods for determining kinetic hydricity

Much of the application of computational methods to kinetic hydricity has been dedicated to specific reactions involving hydride transfer. In fact, the most common computational studies of kinetic hydricity involve the calculation of reaction barriers in catalytic systems, in which hydride transfer is a key step of the mechanism. Typically, traditional DFT methods are used to calculate the barrier for hydride transfer, and good agreement between experiment and theory is observed. In fact, DFT likely has an important role to play in the analysis of ligand effects on kinetic hydricity and in the interpretation of KIEs. To date, it simply has not been used to evaluate kinetic hydricity in a systematic fashion. One area where DFT is currently lacking is in the calculation of solvent effects in kinetic hydricity. The relatively small changes in transition state

energies observed in different solvents and the large computational costs associated with modelling explicit solvent molecules make this a challenge for current DFT methods. Experimental results suggest that this is an important problem to address as rates of hydride transfer correlate better with AN or ET_{30}, which consider specific interactions with the solvent, than with dielectric constant, which considers the solvent as a continuum.

What can be learned from kinetic hydricity

The study of kinetic hydricity originated from researchers wanting to compare and predict hydride transfer rates in order to aid catalyst design. This is still a primary goal of kinetic hydricity studies. For example, in formic acid dehydrogenation reactions (Figure 18a), hydride transfer from the formate ligand to the transition metal (the microscopic reverse of CO_2 insertion into an M–H bond) is often the turnover-limiting step (Figure 18b). Stoichiometric studies of either the decarboxylation reaction directly or the reverse CO_2 insertion can help elucidate electronic or steric effects of the ancillary ligand, which can aid in ligand design for catalysis. Additionally, studies of this type can help in exploring the effect of the metal center if the ligands are kept constant, or guide solvent selection for catalysis if the rate of hydride transfer is measured in different solvents. Nevertheless, given that catalytic reactions involve many steps, the impact of tuning the catalyst for one elementary step in the reaction pathway is not always clear and it is important to understand the nature of the turnover-limiting step in catalysis before trying to improve any individual step.

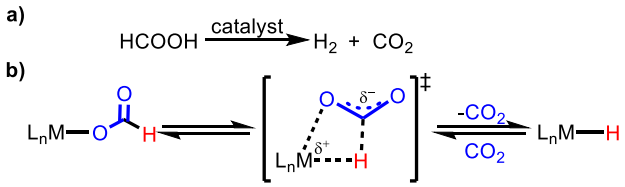

Figure 18. (a) Formic acid dehydrogenation; **(b)** Hydride transfer from the formate ligand to the transition metal is often the turnover-limiting step.

When considering what specifically can be learned from kinetic hydricity measurements, it is informative to consider a case where stoichiometric studies directly assisted in the development of catalysts. A notable example is the design of transition metal catalysts for the ionic hydrogenation of ketones and aldehydes (Figure 19a).[47] In these reactions, H_2 is heterolytically split and then transferred stepwise (as a proton and a hydride) to the substrate. Early work on ionic hydrogenations used a stoichiometric main group hydride (e.g. $HSiEt_3$) and a strong acid (e.g.

trifluoromethanesulfonic acid) to provide the hydride and proton. Transition metal hydrides were identified as promising candidates to perform catalytic hydrogenations, as they could in principle be regenerated from H_2. Therefore, initial attempts were made to perform ionic hydrogenation reactions using a stoichiometric quantity of a transition metal hydride and a strong acid. However, these reactions often gave deleterious side products because of competitive protonation of the transition metal hydride by the strong acid to form H_2 (Figure 20).

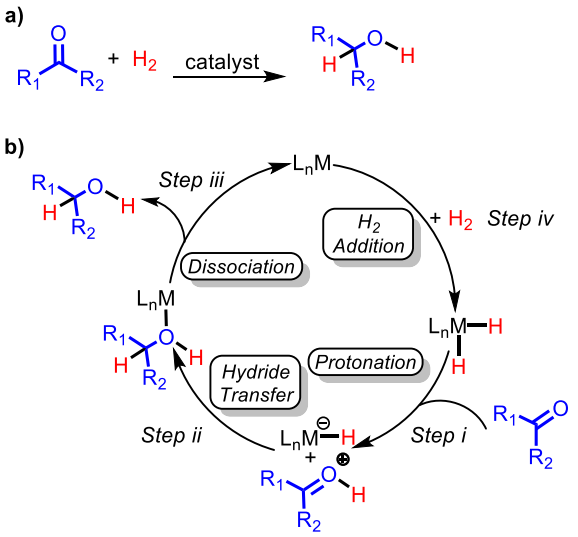

Figure 19. (a) Generic depiction of ketone hydrogenation and **(b)** proposed mechanism for ionic hydrogenation.

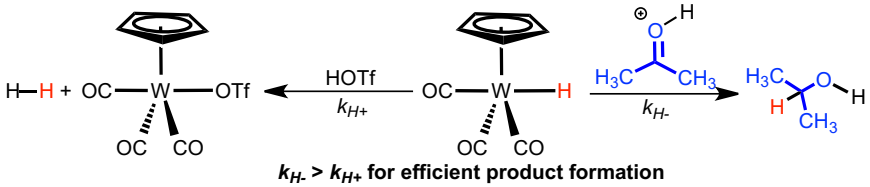

Figure 20. Competing reactions of the hydride in $W(Cp)(CO)_3H$ during stoichiometric ionic hydrogenation of ketones with trifluoromethanesulfonic acid as described in ref. 47.

Studies on kinetic hydricity (many of which we have detailed in the preceding sections) were able to solve the challenge of protonation of the hydride being faster than the rate of hydride transfer. For example, the complex $W(Cp)(CO)_3H$ was found to be highly successful for stoichiometric hydrogenation reactions in part because of the rapid rate of hydride transfer relative to the rate of protonation. Further studies allowed for the development of a complete catalytic cycle. Complexes related to $W(Cp)(CO)_3H$, such as $[W(Cp)(CO)_2(PMe_3)(H)_2]^+$ are highly acidic, allowing them to replace the strong acid and protonate the ketone (Figure 19b, *step i*). The monohydride (formed by deprotonation of the dihydride), $W(Cp)(CO)_2(PMe_3)H$, also undergoes

rapid hydride transfer with the protonated ketone (*step ii*), similar to the tricarbonyl congener. Finally, the product alcohol, which was found to bind to the metal center after hydride transfer (*step iii*), could be displaced easily with H_2 to re-form the starting dihydride complex (*step iv*).

This case study illustrates that the study of kinetic hydricity is most useful when the rates of hydride transfer can be compared to the rates of other hydride transfer reactions or other elementary reactions in a catalytic cycle. In our opinion, it is this type of comparison that will most likely result in kinetic hydricity measurements being used to make important discoveries in catalyst development.

One complication in performing kinetic hydricity studies is that species that are active catalysts may be too unstable to use in stoichiometric studies. In these cases, it may be possible to use model systems with improved stability. For example, a model system was used to elucidate important mechanistic information about hydride transfer from a metal hydride to CO_2 to form a metal formate complex (a CO_2 insertion reaction). Studying the effect of solvent and additives used in catalysis, such as Lewis acids on the insertion of CO_2 into $(({}^{i}Pr_2PCH_2CH_2)_2N)Ir(H)_3$ (a highly active catalyst for CO_2 hydrogenation to formate)[48] is difficult due to the instability of this hydride starting material in coordinating and halogenated solvents (Figure 21a).[34] As a result of these limitations, the model complex [Ru(tpy)(bpy)H][PF_6] (Figure 21b), which inserts CO_2 via an analogous mechanism to the iridium complex but is not catalytically active, was used to perform experiments exploring hydride transfer.[35] This allowed the kinetics of CO_2 insertion to be determined in more polar solvents, such as alcohols, and for the effects of Lewis acids to be determined. The insights gained from the model complex can then be applied to improving the elementary step in catalysis.

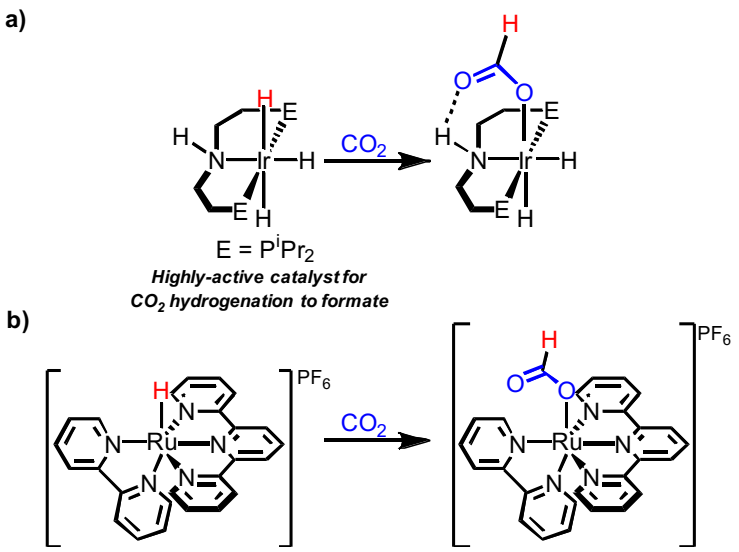

Figure 21. (a) Catalytically relevant CO_2 insertion into an unstable iridium complex and **(b)** model ruthenium complex used in stoichiometric studies for determining information related to kinetic hydricity.

Outlook and challenges

Modern methods of instrumentation, as well as numerical modeling programs, now allow for the collection and interpretation of kinetic data that was previously challenging. Therefore, our ability to measure kinetic hydricity of transition metal hydrides has greatly improved. Future work in the field will likely provide further insights into solvent and ancillary ligand effects on hydride transfer, and address the impact of additives that are commonly used in catalysis, such as Lewis acids on hydride transfer. As researchers become more familiar with measuring kinetic hydricity it would be advantageous for catalyst design if data could be obtained on the rates of hydride transfer using catalytically relevant transition metal hydrides and hydride acceptors. This remains a major challenge for the field, but valuable information can still be gained from model systems.

IV. Connections Between Thermodynamic and Kinetic Hydricity

Despite the plethora of research into both thermodynamic and kinetic hydricity, there are very few cases where *both* thermodynamic and kinetic hydricity measurements have been recorded on the same metal hydride complex. Correlating thermodynamic and kinetic hydricity would result in the creation of linear free-energy relationships (LFERs). As first demonstrated in the physical organic chemistry literature, LFERs provide both empirical predictions (how sensitive the kinetics of hydride transfer are to changes in thermodynamic hydricity) and mechanistic insight (such as

information about the nature of transition states). LFERs are therefore highly valuable tools for catalyst design because once relationships between the kinetic and thermodynamic hydricity of a transition metal hydride are established, it is possible to predict the kinetic reactivity (and in some cases catalytic activity) of metal hydrides based on a single thermodynamic measurement.

Most LFERs involving thermodynamic hydricity have focused on correlations with overall catalytic activity, as measured by TOF or product yield (ideally reflecting an initial rate). For example, it was demonstrated that there is a strong correlation between the TOF of cobalt hydride catalysts for CO_2 hydrogenation to formate and the thermodynamic hydricity of the hydride (Figure 22).[49] Hydride transfer was determined to be the turnover-limiting step, so the LFER provides information on how changes in ΔG^{o}_{H-} affect the rate of hydride transfer, with more hydridic cobalt hydride intermediates reacting more rapidly with CO_2. In fact, the LFER shown in of Figure 22c, indicates that new catalysts with increased thermodynamic hydricity (lower ΔG^{o}_{H-} values) will exhibit higher TOF values compared to current systems. Other LFERs can predict how structural changes will impact ΔG^{o}_{H-}, such as Hammett plots or correlations with steric parameters, which can further guide catalyst development.

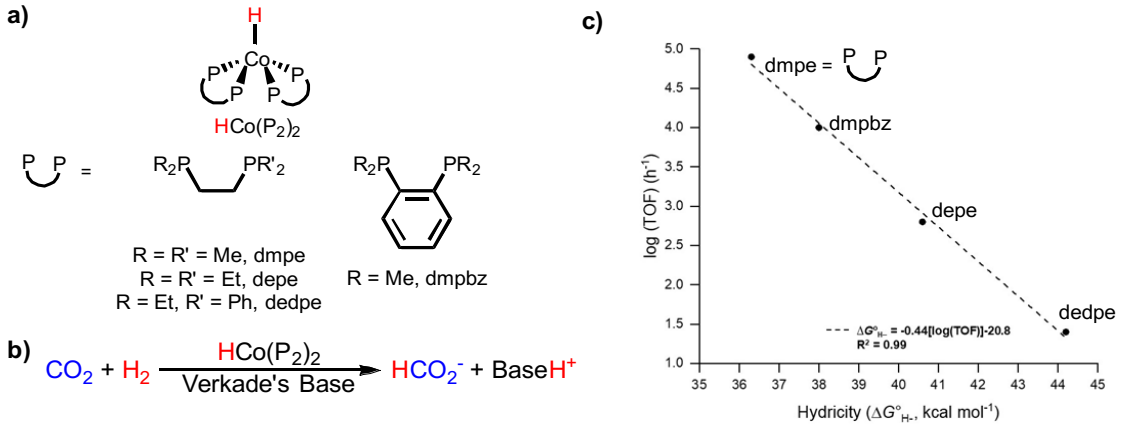

Figure 22: (a) Catalysts and **(b)** reaction for determination of a LFER **(c)** between thermodynamic hydricity and catalyst turnover frequency. Data taken from Table S5 of ref. 49.

Correlating thermodynamic hydricity with catalytic activity will not always be productive. If the turnover-limiting step does not involve hydride transfer, correlations might be weak or non-existent. The turnover-limiting step can also change as the catalyst is changed. In this case, a strong correlation between TOF and ΔG^{o}_{H-} might be observed until a certain point, followed by a discontinuity representing the point at which hydride transfer becomes sufficiently rapid that it is

no longer turnover-limiting. This still provides valuable guidance in catalyst design, as illustrated by a study in which Do and Ngo examined catalytic activity alongside thermodynamic hydricity for a series of Cp*Ir-based hydrides.[50] In this study, electronic tuning of the supporting ligands influenced hydride transfer kinetics more than hydride formation kinetics, leading to a change in the nature of the turnover-limiting step(s) across the series. Furthermore, the span in ΔG^{o}_{H-} values was quite small, complicating efforts to establish systematic correlations.

Considering the challenges of correlating thermodynamic hydricity with full catalytic reactions, correlations between kinetic hydricity (measured as an individual stoichiometric process to a well-defined acceptor) and thermodynamic hydricity are expected to be highly valuable. Such LFERs are likely to be relevant to *many* reactions that involve hydride transfer, instead of one specific catalytic reaction. However, such detailed studies are almost entirely lacking. Our non-controversial hypothesis is that as a hydride becomes more hydridic (smaller ΔG^{o}_{H-}), the kinetic rate of hydride transfer will increase according to the Evans-Polanyi principle (Figure 23a). This has been qualitatively demonstrated separately by Bullock and Bruno in measurements of hydride transfer to substituted trityl cations.[32,43] We further hypothesize that the details of the LFER, such as the slope of the correlation and its temperature- and solvent-dependent behavior, will provide key mechanistic insights that will be broadly valuable in altering the properties of a class of metal hydrides. For instance, changing the solvent may make a specific reaction more thermodynamically favorable but less kinetically favorable (Figure 23b). Due to the limited number of studies into thermodynamic hydricity in different solvents this question remains to be answered, but may be valuable for optimizing solvent choice in catalytic reactions.

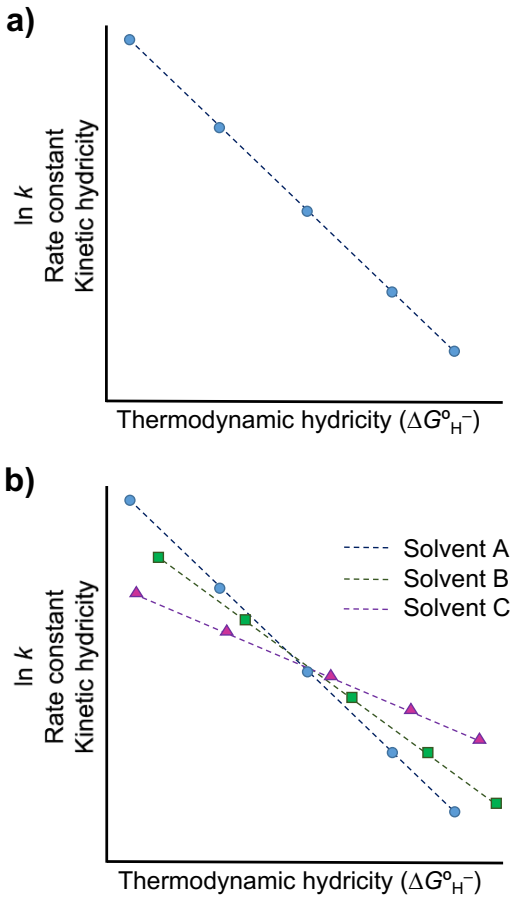

Figure 23: Hypothetical representations of **(a)** a scaling relationship between kinetic and thermodynamic hydricity and **(b)** how the relationship may differ between solvents. Shapes represent data points for different complexes. Dotted lines represent hypothetical scaling relationship between thermodynamic hydricity and rate constant for hydride transfer (kinetic hydricity).

A seminal example compiling individual hydride transfer kinetics and thermodynamic hydricity comes from Creutz and co-workers' study of $[Ru(tpy)(bpy)H]^+$. Of particular note, the study compared the rate of hydride transfer to several different pyridinium acceptors, a number of transition metal acceptors, and CO_2 in acetonitrile.[22] Such studies are important because they can identify acceptor-specific anomalies in the kinetic behavior, such as complicating steric effects, that provide a more general understanding of the relationship between kinetic and thermodynamic hydricity. The Creutz study also illustrates some of the challenges in correlating thermodynamic and kinetic hydricity. Reactions with some sets of hydride acceptors had quantifiable kinetics, but similar thermodynamic hydricities; other reactions suffered from poor solubility that prevented measurements of kinetic hydricity in the same solvent as the thermodynamic hydricity

measurements. This prevented a comprehensive analysis of the correlation of rates of hydride transfer and the thermodynamic driving force for hydride transfer under consistent conditions. In general, it is not straightforward to find systems that meet the individual criteria for measuring either thermodynamic or kinetic hydricity (see sections II and III), let alone satisfy both sets of requirements. The development of methods to measure thermodynamic hydricity in a greater range of solvents may be ground-breaking in this regard and we expect that it should now be possible to find transition metal complexes where both kinetic and thermodynamic hydricity can be measured.

Overall, although it is certainly the case that individual measurements of thermodynamic and kinetic hydricity, as well as correlations between them, will be valuable, they will not necessarily be a panacea for catalyst design. Even though hydride transfer is often an elementary step in catalysis, it is not always the turnover-limiting step, and in these cases increasing the rate of hydride transfer will not have a major effect on catalytic performance. Similarly, in hydrogenation and dehydrogenation reactions that proceed via a mechanism involving metal-ligand cooperation, hydricity is unlikely to be an important factor as hydride transfer is no longer a discrete elementary step. (A change in correlation with ΔG^{o}_{H-} could, however, indicate a change in mechanism from a stepwise to concerted TS.) Nevertheless, there are enough reactions where direct hydride transfer from a metal center is the crucial step in catalysis that information about thermodynamic and kinetic hydricity will prove important in designing new and improved systems. In conclusion, this Tutorial highlights methods to make measurements of thermodynamic and kinetic hydricity and we are optimistic that it will encourage more researchers to report these values, which will increase the power of approaches based on thermodynamic and kinetic hydricity.

Supporting Information

Thermochemical derivations (PDF)

Complete table and charts of thermodynamic hydricity values (XLS)

Number-line chart of thermodynamic hydricity in acetonitrile (PDF)

Number-line chart of thermodynamic hydricity in water (PDF)

Acknowledgements

The thermodynamic hydricity aspects were supported by the U.S. Department of Energy, Office of Science, Office of Basic Energy Sciences, under Award No. DE-SC0014255. The kinetic hydricity aspects were supported by the National Science Foundation through Grant CHE-1953708.

References

1 M. Rakowski DuBois and D. L. DuBois, *Acc. Chem. Res.*, 2009, **42**, 1974–1982.

2 E. S. Wiedner, M. B. Chambers, C. L. Pitman, R. M. Bullock, A. J. M. Miller and A. M. Appel, *Chem. Rev.*, 2016, **116**, 8655–8692.

3 S. Ilic, A. Alherz, C. B. Musgrave and K. D. Glusac, *Chem. Soc. Rev.*, 2018, **47**, 2809–2836.

4 K. M. Waldie, A. L. Ostericher, M. H. Reineke, A. F. Sasayama and C. P. Kubiak, *ACS Catal.*, 2018, **8**, 1313–1324.

5 A. Dedieu, Ed., *Transition Metal Hydrides*, VCH Publishers, New Y, 1992.

6 D. E. Berning, B. C. Noll and D. L. DuBois, *J. Am. Chem. Soc.*, 1999, **121**, 11432–11447.

7 S. J. Connelly, E. S. Wiedner and A. M. Appel, *Dalton Trans.*, 2015, **44**, 5933–5938.

8 C. Tsay, B. N. Livesay, S. Ruelas and J. Y. Yang, *J. Am. Chem. Soc.*, 2015, **137**, 14114–14121.

9 K. R. Brereton, C. N. Jadrich, B. M. Stratakes and A. J. M. Miller, *Organometallics*, 2019, **38**, 3104–3110.

10 C. P. Andrieux, I. Gallardo, J. M. Savéant and K. B. Su, *J. Am. Chem. Soc.*, 1986, **108**, 638–647.

11 A. A. Isse and A. Gennaro, *J. Phys. Chem. B*, 2010, **114**, 7894–7899.

12 R. H. Morris, *Chem. Rev.*, 2016, **116**, 8588–8654.

13 C. L. Pitman, K. R. Brereton and A. J. M. Miller, *J. Am. Chem. Soc.*, 2016, **138**, 2252–2260.

14 G. Kovács and I. Pápai, *Organometallics*, 2006, **25**, 820–825.

15 J. T. Muckerman, P. Achord, C. Creutz, D. E. Polyansky and E. Fujita, *Proc. Natl. Acad. Sci.*, 2012, **109**, 15657–15662.

16 X.-J. J. Qi, Y. Fu, L. Liu and Q.-X. X. Guo, *Organometallics*, 2007, **26**, 4197–4203.

17 K. R. Brereton, S. M. Bellows, H. Fallah, A. A. Lopez, R. M. Adams, A. J. M. Miller, W. D. Jones and T. R. Cundari, *J. Phys. Chem. B*, 2016, **120**, 12911–12919.

18 S. Chen, R. Rousseau, S. Raugei, M. Dupuis, D. L. DuBois and R. M. Bullock, *Organometallics*, 2011, **30**, 6108–6118.

19 M. Besora, P. Vidossich, A. Lledós, G. Ujaque and F. Maseras, *J. Phys. Chem. A*, 2018, **122**, 1392–1399.

20 C. P. Kelly, C. J. Cramer and D. G. Truhlar, *J. Phys. Chem. B*, 2006, **110**, 16066–16081.

21 C. Creutz and M. H. Chou, *J. Am. Chem. Soc.*, 2009, **131**, 2794–2795.

22 Y. Matsubara, E. Fujita, M. D. Doherty, J. T. Muckerman and C. Creutz, *J. Am. Chem. Soc.*, 2012, **134**, 15743–15757.

23 B. M. Ceballos, C. Tsay and J. Y. Yang, *Chem. Commun.*, 2017, **53**, 7405–7408.

24 S. I. Johnson, R. J. Nielsen and W. A. Goddard, *ACS Catal.*, 2016, **6**, 6362–6371.

25 B. M. Ceballos and J. Y. Yang, *Proc. Natl. Acad. Sci.*, 2018, **115**, 12686–12691.

26 B. M. Ceballos and J. Y. Yang, *Organometallics*, 2020, **39**, 1491–1496.

27 D. W. Cunningham, J. M. Barlow, R. S. Velazquez and J. Y. Yang, *Angew. Chem. Int. Ed.*, 2020, **59**, 4443–4447.

28 S. A. Burgess, A. M. Appel, J. C. Linehan and E. S. Wiedner, *Angew. Chem. Int. Ed.*, 2017, **56**, 15002–15005.

29 M. S. Jeletic, M. T. Mock, A. M. Appel and J. C. Linehan, *J. Am. Chem. Soc.*, 2013, **135**, 11533–11536.

30 T.-Y. Cheng, B. S. Brunschwig and R. M. Bullock, *J. Am. Chem. Soc.*, 1998, **120**, 13121–13137.

31 U. L. Gunther, in *Topics in Current Chemistry*, 2013, pp. 23–70.

32 T.-Y. Cheng and R. M. Bullock, *Organometallics*, 2002, **21**, 2325–2331.

33 T.-Y. Cheng and R. M. Bullock, *Organometallics*, 1995, **14**, 4031–4033.

34 J. E. Heimann, W. H. Bernskoetter and N. Hazari, *J. Am. Chem. Soc.*, 2019, **141**, 10520–10529.

35 J. E. Heimann, W. H. Bernskoetter, N. Hazari and J. M. Mayer, *Chem. Sci.*, 2018, **9**, 6629–6638.

36 I. A. Kieffer, N. R. Treich, J. L. Fernandez and Z. M. Heiden, *Dalton Trans.*, 2018, **47**, 3985–3991.

37 W. W. Ellis, J. W. Raebiger, C. J. Curtis, J. W. Bruno and D. L. DuBois, *J. Am. Chem. Soc.*, 2004, **126**, 2738–2743.

38 T. Y. Cheng and R. M. Bullock, *J. Am. Chem. Soc.*, 1999, **121**, 3150–3155.

39 M. Gómez-Gallego and M. A. Sierra, *Chem. Rev.*, 2011, **111**, 4857–4963.

40 G. Parkin, *Acc. Chem. Res.*, 2009, **42**, 315–325.

41 L. M. Slaughter, P. T. Wolczanski, T. R. Klinckman and T. R. Cundari, *J. Am. Chem. Soc.*, 2000, **122**, 7953–7975.

42 B. P. Sullivan and T. J. Meyer, *Organometallics*, 1986, **5**, 1500–1502.

43 N. Sarker and J. W. Bruno, *J. Am. Chem. Soc.*, 1999, **121**, 2174–2180.

44 H. Konno, A. Kobayashi, K. Sakamoto, F. Fagalde, N. E. Katz, H. Saitoh and O. Ishitani, *Inor. Chim. Acta*, 2000, **299**, 155–163.

45 C. Reichardt, *Angew. Chem. Int. Ed.*, 1979, **18**, 98–110.

46 C. Creutz, M. H. Chou, H. Hou and J. T. Muckerman, *Inorg. Chem.*, 2010, **49**, 9809–9822.

47 R. M. Bullock, *Chem. – A Eur. J.*, 2004, **10**, 2366–2374.

48 T. J. Schmeier, G. E. Dobereiner, R. H. Crabtree and N. Hazari, *J. Am. Chem. Soc.*, 2011, **133**, 9274–9277.

49 M. S. Jeletic, E. B. Hulley, M. L. Helm, M. T. Mock, A. M. Appel, E. S. Wiedner and J. C. Linehan, *ACS Catal.*, 2017, **7**, 6008–6017.

50 A. H. Ngo and L. H. Do, *Inorg. Chem. Front.*, 2020, **7**, 583–591.